Pergamon

Geochimica et Cosmochimica Acta, Vol. 60, No. 18, pp. 3487–3504, 1996

0016-7037/96 $15.00 + .00

PII S0016-7037(96)00182-2

Oxygen isotope record of fluid infiltration and mass transfer during regional metamorphism of pelitic schist, Connecticut, USA

JOOST L. M. VAN HAREN,* JAY J. AGUE, and DANNY M. RYE
Department of Geology and Geophysics, Yale University, New Haven, CT 06520-8109, USA

(*Received October* 20, 1995; *accepted in revised form May* 20, 1996)

Abstract—We present petrologic and oxygen isotopic evidence for the interaction of deep crustal fluids with kyanite zone pelitic schist during amphibolite facies metamorphism of the Wepawaug Schist, south-central Connecticut. We focus on a sample of schist (sample MBW-1) cut by a 2–6 cm wide quartz vein. The vein is surrounded by zones of wallrock alteration (selvages) that are rich in micas relative to quartz and feldspar, have low Si/Al and Na/Al, contain staurolite and kyanite, and vary in thickness from about 1–5 cm. Staurolite and kyanite are rare or absent beyond the selvage margins. We have measured the $\delta^{18}O$ of quartz, plagioclase, muscovite, garnet, kyanite, staurolite, garnet, and biotite along several mm-scale resolution traverses across the quartz vein and the adjacent schist. Garnets in the selvages record core-to-rim increases in $\delta^{18}O$ of nearly 2‰. Modeling of prograde reaction histories indicates that this zonation requires the infiltration of external fluids. Beyond the selvage margins, isotopic zonation in garnet is about 0.8‰ from core-to-rim and is consistent with prograde reaction with little or no infiltration. We suggest, therefore, that the selvages were zones of significant fluid infiltration and that the region now occupied by the quartz vein was the major fluid conduit. Earlier petrologic studies (Ague, 1994b) indicated that quartz veins and adjacent selvages were conduits for major down-temperature flow of H_2O-rich fluids with time-integrated fluid fluxes of $\sim 3 \times 10^5$ m^3 m^{-2}. Isotopic modeling of advective flow suggests that down-temperature fluxes of this magnitude would have increased bulk $\delta^{18}O$ by ~1‰, consistent with the isotopic record preserved by zoned selvage garnets. Quartz in veins surrounded by selvages from five other localities throughout the amphibolite facies have $\delta^{18}O$ that is statistically indistinguishable from that of the bulk of the quartz in MBW-1. Thus, we conclude that the amphibolite facies portion of the Wepawaug Schist was a zone of major, channelized outflow of metamorphic fluids down the regional temperature gradient.

During the latter stages of amphibolite facies metamorphism subsequent to the bulk of vein and selvage formation, MBW-1 was infiltrated by isotopically light fluids that were probably derived from synmetamorphic igneous intrusions. This infiltration modified the isotopic composition of plagioclase throughout the rock and, therefore, we suggest that the infiltration was pervasive. Muscovite retains its pre-infiltration isotopic composition, however, which suggests short timescales of fluid-rock interaction on the order of 10^3–10^4 years. The total duration of flow may have been longer than this because our calculations do not take episodic flow into account.

Modeling of possible isotopic shifts resulting from diffusion of oxygen isotopes between matrix phases during slow cooling indicates that MBW-1 must have been dry for most of its retrograde cooling history.

1. INTRODUCTION

Quartz veins are abundant in regional metamorphic belts worldwide (cf. Vidale, 1974; Walther and Orville, 1982; Yardley, 1986), but their origins and their role in crustal heat and mass transfer remain controversial. Two contrasting hypotheses have been advanced to account for metamorphic vein genesis. One hypothesis holds that veins form by local mass transfer in which silica is extracted from wallrocks by processes such as diffusion and then deposited in adjacent fractures (e.g., Yardley, 1975; Yardley and Bottrell, 1992). The other holds that veins represent conduits for major channelized fluid transport down regional temperature and pressure gradients (e.g., Walther and Orville, 1982; Ferry and Dipple, 1991; Ferry, 1992). For the case of local mass transfer, large time-integrated fluid fluxes are not required to form veins. In contrast, vein formation by channelized flow requires immense time-integrated fluxes that have the potential to transport both mass and heat during metamorphism (cf. Rye et al., 1976; Bickle and McKenzie, 1987; Tracy et al., 1983; Chamberlain and Rumble, 1988; Ferry and Dipple, 1991; Hoisch, 1991; Palin, 1992; Ague, 1994b, 1995a,b).

One of the most controversial aspects of the problem is whether quartz vein formation produces significant metasomatic alteration of adjacent wallrocks (e.g., Ague, 1995b; Walther and Holdaway, 1995). Ague (1994a,b) concluded that channelized fluid flow was a major control on the chemical and mineralogic evolution of amphibolite facies metapelitic rocks of the Wepawaug Schist, Connecticut. On the regional scale, the intensity of metasomatism of the schists is closely related to vein density. Vein density increases from 2–4 vol% in the lowest grade rocks to about 20–30 vol% in the kyanite zone. Amphibolite facies quartz veins are commonly surrounded by a highly aluminous selvage rich in staurolite ± kyanite and micas and poor in quartz and plagioclase, whereas staurolite and kyanite are typically absent from less aluminous wallrocks located beyond the sel-

* *Present address:* Biosphere 2, P.O. Box 689, Oracle, AZ 85623, USA.

vage margins. On the basis of local and regional scale mass balance including wallrocks and veins, Ague (1994a,b) concluded that pelitic schist lost large amounts of silica and volume at the hand sample scale as a result of local scale mass transfer from wallrocks into opening fractures. This silica loss, however, can only account for about 70% of the total volume of quartz in the average amphibolite facies vein. The other 30% was inferred to have been derived from the regional scale, down-temperature flow of fluids through fractures. The large fluid fluxes required to deposit the externally-derived quartz led to loss of alkali metals (particularly Na), alkaline earth metals, and P, and gain of Cu, Mn, and Zn in the selvages adjacent to the veins. In addition, some schists gained K and Ba. The alkali mass transfer was particularly important petrologically because it helped to stabilize staurolite ± kyanite in the selvages.

In this paper, we use stable isotopic and petrologic methods to assess the mechanisms and timing of the interaction of deep crustal fluids with kyanite zone metapelitic rocks of the Wepawaug Schist and to test further the hypothesis that the quartz veins represent regional fluid outflow conduits. We have measured the $\delta^{18}O$ of quartz, plagioclase, muscovite, garnet, kyanite, staurolite, garnet, and biotite along several high spatial resolution traverses across a sample of quartz vein and adjacent pelitic schist. These data provide unique constraints on fluid-rock interaction because the isotopic systematics of all coexisting silicate phases can be examined within a well defined spatial framework. We pay particular attention to the isotopic systematics of garnet because recent studies have shown that this phase can preserve a detailed record of fluid infiltration events during both prograde and retrograde metamorphism (cf. Chamberlain and Conrad, 1991, 1993; Kohn, 1993; Young, 1993; Young and Rumble, 1993; Kohn and Valley, 1994). Furthermore, we have measured the oxygen isotopic composition of a number of quartz veins throughout the Wepawaug Schist to better understand regional flow processes and fluid sources.

2. OVERVIEW OF REGIONAL GEOLOGY AND PREVIOUS ISOTOPIC STUDIES

The Wepawaug Schist forms part of the Orange-Milford Belt of South Central Connecticut (Fig. 1; Rodgers, 1985) and consists mainly of metamorphosed pelitic and psammitic schists but includes some metacarbonate and felsic metavolcanic horizons. Small (~0.1–200 m wide) dikes and pods of leucocratic igneous rocks intruded the central-western part of the Schist (Fritts, 1965a; Ague, 1994b). Fritts (1962) concluded that the sediments were deposited during the Siluro-Devonian and correlated them with the Waits River and Northfield Formations of Vermont. Metamorphic grade increases from chlorite to kyanite zone from east-to-west across the Schist (Fig. 1; Fritts, 1963, 1965a,b). Peak temperatures ranged from ~400 to ~600–650°C from the chlorite to the kyanite zone, and peak pressures were ~0.8 ± 0.1 GPa (Ague, 1994b). The structural and stratigraphic arguments of Dieterich (1968) and the geochronologic results of Palin and Seidemann (1990), Lanzirotti and Hanson (1992), and Lanzirotti et al. (1995) suggest that prograde metamorphism occurred during the Acadian orgeny (~420–360 Ma; Gates, 1975; Osberg et al., 1989; Armstrong et al., 1992). The regional penetrative cleavage overprints an earlier foliation(s), marks the axial planes of folds in bedding and quartz veins, strikes north-northeast, and dips steeply to the west in the eastern part of the Schist and steeply to the east in the western part (cf. Fritts, 1963, 1965a,b; Dieterich, 1968; Ague, 1994b). Fritts (1963, 1965a,b) and Dieterich (1968) concluded that the rocks of the Orange-Milford belt were deformed into a major north-northeast plunging synformal syncline (Fig. 1).

Previous stable isotopic studies have focused mainly on the Wepawaug carbonates (e.g., Tracy et al., 1983; Palin, 1992; Palin and Rye, 1992). Tracy et al. (1983) found that infiltration of ^{18}O-depleted fluids through fractures (now quartz veins) during amphibolite facies metamorphism drove mineral reactions and caused major decreases in bulk $\delta^{18}O$, $\delta^{13}C$, K/Al, Na/Al, Ca/Al, Mg/Fe, and volume in adjacent marble. Palin (1992) and Palin and Rye (1992) showed that amphibolite facies marbles throughout the Wepawaug Schist had undergone varying degrees of infiltration by water-rich fluids at or near peak metamorphic conditions, consistent with the earlier petrologic results of Hewitt (1973). Fluid flow was probably in a down-temperature direction (Palin and Rye, 1992).

3. SAMPLES

Oxygen isotope profiles, mineral chemistry determinations, and textural analyses were done for the quartz vein and adjacent pelitic wallrock of kyanite zone sample MBW-1 (Fig. 1). We also determined the bulk $\delta^{18}O$ of five quartz veins cutting pelitic schists and two quartz veins associated with leucocratic intrusions collected from other amphibolite facies localities in the Wepawaug Schist (Fig. 1).

The outcrop from which MBW-1 was collected covers an area of ~60 m^2 and consists of pelitic schist and quartz veins with minor amphibolite and tonalite. Quartz veins comprise ~21 vol% of the outcrop (Ague, 1994b). Based on measurements of fifteen quartz veins, vein width varies between ~0.5 and ~6.0 cm and averages ~1.3 cm. Most veins are tightly folded and the fold limbs are boudinaged to varying degrees.

A large (~2 to ~6 cm wide) quartz vein is folded around MBW-1 (Fig. 2a,b). A ~2 to ~8 cm wide aluminous zone or selvage analogous to those described by Ague (1994b) is present adjacent to the vein. The selvage contains abundant micas, staurolite, kyanite, graphite, and Fe-Ti oxides, but is poor in quartz and plagioclase (Table 1). Beyond the selvage margins, quartz and plagioclase are considerably more abundant and staurolite and kyanite are rare or absent (Table 1). Tourmaline, apatite, zircon, and sulfides are widespread accessory phases throughout the rock. Major element zoning profiles for garnets within and outside the selvages are nearly identical within measurement error. Small quartz veinlets ~2 to ~8 mm wide and <5 cm long cut the schist (Fig. 2a,b). The axial planes of folds in the large quartz vein and the veinlets are subparallel to the schistosity. Kyanite crystals form a strong lineation that is subparallel to the fold axes.

The bulk $\delta^{18}O$ of quartz from veins surrounded by aluminous selvages was determined for five additional amphibolite facies pelitic schists to assess regional isotopic variations (samples JAW-122, -125A, -131A, -137B, and W-12; Fig. 1) (see Ague, 1994b, for detailed discussion).

The isotopic compositions of quartz from two veins associated with syn-orogenic intrusive rocks were determined to constrain fluid compositions associated with magmas (samples JvH-W-14 and JAW-89; Fig. 1). Both outcrops consist mainly of pelitic schist, quartz veins, and dikes and irregularly shaped pods of leucocratic igneous rocks. Granitic, aplitic, and pegmatitic textures are common in the igneous rocks. Sample JvH-W-14 is from an aplite dike and consists of quartz, plagioclase, muscovite, and rare garnet. The analyzed quartz was taken from a small (~0.5 cm wide) quartz

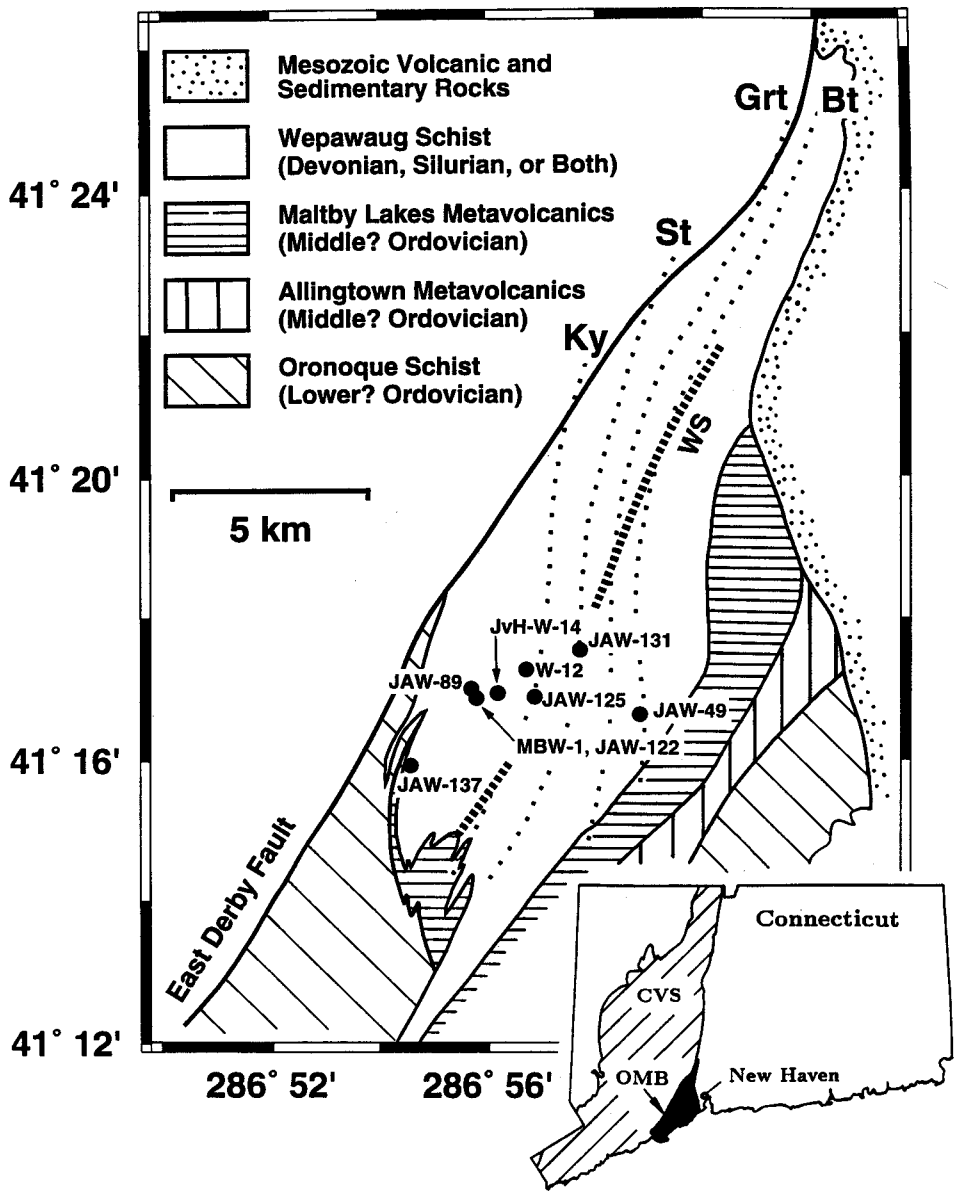

FIG. 1. Generalized geologic map of the Orange-Milford belt of south-central Connecticut (modified from Fritts, 1962a, 1963, 1965a,b; Dieterich, 1968; Rodgers, 1985) and sample locations. Isograd locations modified from Fritts (1963, 1965a,b) by Ague (1994a). WS: axis of the Wepawaug syncline. The position of the Orange-Milford belt (OMB) in the Connecticut Valley Synclinorium (CVS) is shown on the inset location map.

vein within the dike. JAW-89 is a 6 cm wide, coarse-grained (~1–2 cm crystals), quartz-plagioclase vein that emanates from a granitic dike and cuts pelitic schist.

4. METHODS

4.1. Samples For Stable Isotope Analysis

Sample MBW-1 was cut into several 2.5 cm thick slabs perpendicular to vein-wallrock contacts and fold axes. Based on macroscopic observations, two slabs were selected for detailed isotopic work.

Traverse A-A′ extends from the vein-wallrock contact across the selvage into the less aluminous wallrock beyond the selvage margins (Fig. 2a). Eleven rectangular samples of rock were cut out along the traverse using a low speed precision saw with a 0.15 mm thick blade and a standard rock saw. The samples had square cross-sections (6 mm or 8 mm on a side) and were 2.5 cm long. The samples were crushed in a vice and then gently ground in an agate mortar to an average particle size of 125–180 μm. Heavy liquids and a Frantz magnetic separator were used to prepare mineral separates that were then purified by handpicking under a binocular microscope. Plagioclase and quartz could not be distinguished based on physical properties. The fraction containing both minerals was, therefore, treated according to the method of Bailey and Stevens (1960), which stains plagioclase red. After staining, quartz and plagioclase were separated by handpicking. Dilute HCl was then used to remove the stain from the plagioclase grains.

Garnet core and rim separates were obtained using two different methods. The first method is based on the observation that garnet crystals in the selvage have predominantly clear, inclusion-free cores whereas the rims contain ~3 modal % Fe-Ti oxide inclusions and

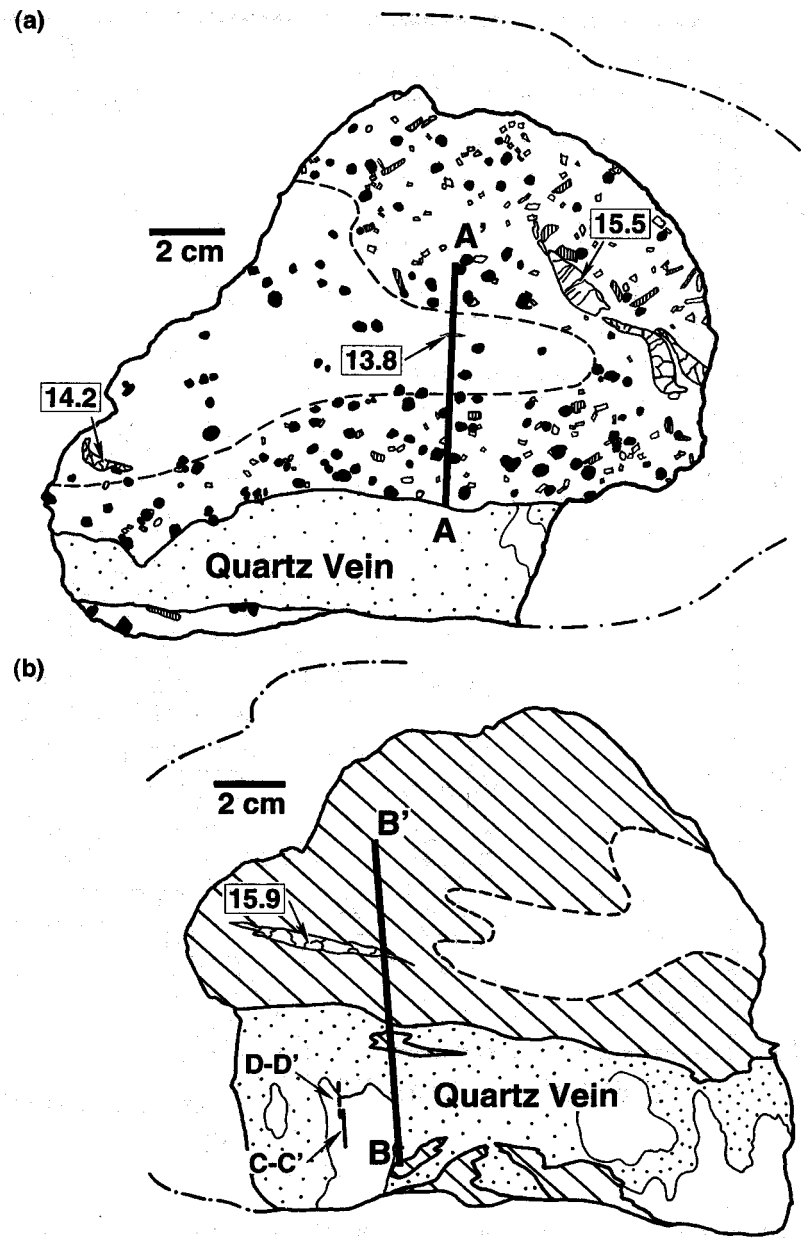

FIG. 2. Rock slabs (cut from MBW-1) used to prepare samples for oxygen isotope traverses. Slabs cut perpendicular to fold axes. (a) Traverse A-A′. Macroscopically observable limit of aluminous selvage denoted by dashed line. Symbols used for porphyroblasts are black: garnet; vertical rule: staurolite; open: kyanite. Regions in quartz vein shown with stipple pattern are composed predominantly of fine-grained, recrystallized quartz; unpatterned regions are composed of coarse-grained (cm scale) quartz crystals. Boxed numbers denote the $\delta^{18}O$ of quartz from small veinlets (in ‰ relative to V-SMOW). Some parts of the large quartz vein could not be extracted successfully from the outcrop; the original extent of the vein is denoted by the heavy dash-dot line. (b) Traverses B-B′, C-C′, and D-D′. Traverse D-D′ is parallel to C-C′ and lies 1.3 cm below the surface of the rock slab. Aluminous selvage denoted by diagonal rule, all other symbols as in Fig. 2a. Note inclusions of wallrock incorporated into vein.

abundant graphite (see Fig. 9 in Ague, 1994b). Major element zoning profiles, determined by electron microprobe, are smooth and continuous across core-rim boundaries. Fragments of garnet core and garnet rim could be easily identified because rim fragments are much darker (owing to graphite inclusions) than core fragments. Garnet core and rim separates were prepared by handpicking the fragments under a binocular microscope; great care was taken to avoid inclusions of quartz and Fe-Ti oxides. Outside the selvage, the inclusion density in garnets does not vary systematically and, thus, a different method was used to prepare core and rim separates. A thin rock slice (~1 mm thick) was cut from the zone outside the selvage directly adjacent to Traverse A-A′. The largest garnet in the slice (3 mm diameter) was selected for analysis. Four ~0.8 mm^3 samples were cut from the garnet along a traverse that passed through the center of the crystal. This procedure yielded two samples of the garnet core and two samples of the rim. The samples were individually ground in an agate mortar and hand-picked to remove quartz and Fe-Ti oxide inclusions.

TABLE 1. MODES (MOLES LITER^{-1})

Mineral	MBW-1 Selvage	MBW-1 Outside selvage	Calculated Protolith
Quartz	3.870	15.400	14.505
Plagioclase	0.664	1.527	1.726
Muscovite	3.002	1.206	1.497
Biotite	1.977	1.746	1.384
Chlorite	-	-	0.299
Garnet	0.576	0.453	-
Staurolite	0.016	-	-
Kyanite	0.952	-	-
Ilmenite	0.361	0.188	0.415
Rutile	0.154	0.085	0.016

The isotopic differences that we measured between garnet cores and rims are probably minimum estimates of the total isotopic zontation in garnet for two reasons. First, the mechanical methods used to obtain garnet separates allow us to determine bulk core and rim compositions, but not the compositions at the centers and outermost edges of the crystals. Second, contamination of $\delta^{18}O$ measurements due to incomplete removal of Fe-Ti oxide inclusions from selvage garnet rims would cause the true rim $\delta^{18}O$ to be underestimated slightly (<0.15‰).

Traverse B-B′ extends across the large quartz vein and the aluminous selvage (Fig. 2b). A 0.5 cm diameter, water-cooled diamond drill was used to obtain 2.5 cm long drill cores spaced ~0.5 cm apart along the traverse. Mineral separates were prepared from the cores using the techniques described above. In addition, to obtain a two-dimensional view of isotopic variations within the vein, quartz separates were prepared from the top, center, and bottom thirds of some of the vein cores.

Traverses C-C′ and D-D′ were done to obtain a mm-scale picture of isotopic variations across individual crystals of vein quartz (Fig. 2b). A rectangular block was sawed from the vein. For Traverse C-C′, a low speed precision saw (0.15 mm thick blade) was used to make cuts spaced ~1 mm apart into one edge of the block. Additional cuts were made to remove the incized edge, and ~1 mm^3 samples of quartz were broken off from the edge using precision pliers. Samples for Traverse D-D′ were prepared from a different part of the rectangular block using the same techniques (Fig. 2b). Traverse C-C′ is 1.2 cm long and consists of 9 ~1 mm^3 quartz samples, whereas D-D′ is 1.1 cm long and consists of five ~1 mm^3 samples.

In addition to the traverses, several samples of quartz from veinlets and pelitic schist adjacent to veinlets were prepared using the methods employed for Traverse A-A′ (Fig. 2a,b).

We also determined the $\delta^{18}O$ of 0.5–1.0 cm^3 bulk samples of quartz veins from five other pelitic rocks (JAW-122, -125A, -131A, -137B, and W-12) and two quartz veins associated with syn-metamorphic intrusions (JvH-W-14, JAW-89).

4.2. Oxygen Isotope Analyses

Oxygen was extracted using a standard BrF_5 line (Clayton and Mayeda, 1963) and converted to CO_2 with a resistance heated graphite rod in the presence of platinum (Taylor et al., 1962). Isotope ratios were measured on a Finnigan Mat 251 mass spectrometer at Yale University and are reported using the usual δ notation relative to V-SMOW. The mass of the analyzed mineral material varied between 0.6 and 10 mg. Samples of garnet and other refractory minerals were ground to a powder to ensure complete reaction (cf. Garlick and Epstein, 1967).

Special care was taken to minimize contamination by atmospheric H_2O. Samples of all phases except plagioclase were loaded into their reaction vessels in a drybox at relative humidities <25% and prefluorinated at 150° for two hours. Plagioclase samples cannot be prefluorinated and, therefore, they were loaded under very low relative humidities <20% to minimize contamination.

Replicate analyses of NBS-28 quartz yield 9.7 ± 0.21‰ (1σ sample standard deviation). We also did replicate analyses of an internal quartz standard (JAQ) prepared from the veins described by Ague (1995a). The precision for this standard is ±0.16‰ and is somewhat better than that observed for NBS-28. We conclude that JAQ is isotopically more homogeneous than our batch of NBS-28, and take ±0.16‰ to be the best estimate of analytical precision for our isotopic analyses for all phases except kyanite.

Oxygen isotope analysis of kyanite is problematic because this mineral is extremely refractory. To determine the optimal conditions for oxygen extraction from kyanite, we ran a series of twenty-eight test extractions using coarse-grained kyanite from the kyanite-sillimanite schist member of the Hartland Formation exposed on Ratlum Mountain, northwestern Connecticut (cf. Schnabel, 1975). Run times were 12–20 hours and run temperatures were 550–720°C. Oxygen yields were a strong positive function of run temperature; yields were <40% at temperatures less than 650°C and reached 85% at 720°C. For yields >40%, $\delta^{18}O$ is uncorrelated with yield and, thus, the kyanite dissolution was probably congruent, or nearly so. The average and sample standard deviation of the data for the >40% yield runs are 12.6 and 0.31, respectively. This standard deviation is greater than that observed for our quartz standards and may be due to either our experimental method or isotopic heterogeneity in the kyanite crystals. We added powdered NaBr to some of the runs in an attempt to produce cryolite during the reaction and thereby increase oxygen yields. X-ray diffraction analysis of the residue remaining after reaction confirms that minor cryolite was made in these runs, but no systematic increase in oxygen yields was observed. The MBW-1 kyanite samples for this study were all run with excess NaBr at temperatures of 720–750°C; oxygen yields varied from 85% to 93%.

4.3. Mineral Compositions, Abundances, and Grain Sizes

Mineral compositions were determined using the fully automated JEOL JXA-8600 electron microprobe in the Department of Geology and Geophysics at Yale University. Accelerating voltage and beam current were 15 kV and 20 nA, respectively. Quantitative analyses used natural and synthetic standards, wavelength dispersive spectrometers, off-peak background corrections, and ZAF matrix corrections. Feldspars and micas were analyzed using a slightly defocused (5 μm diameter) electron beam to prevent alkali loss; analyses of all other phases were done with a focused beam.

Modal analyses were done using the line integration method and a semi-automated digitizing petrographic microscope (Brimhall, 1979). Mineral grain sizes were estimated by averaging the measurements of at least ten of the largest grains of each phase of interest observed in thin section. Modes were converted to mineral moles liter^{-1} using the measured mineral compositions, linear composition-volume relations, and the molar volume data of Berman (1991), Hewitt and Wones (1975), McOnie et al. (1975), and Holdaway et al. (1995).

Mineral abbreviations follow Kretz (1983).

5. QUARTZ VEIN TEXTURES

5.1. Petrographic Observations

Petrographic observations were used to constrain the mechanisms and relative timing of vein formation and deformation in sample MBW-1.

Coarse-grained ovoid or irregularly shaped areas (Fig. 2b) that contain large quartz crystals as much as 2.5 cm long typically occur in the widest parts of the major quartz vein. The crystals are characterized by a mosaic texture (e.g., Spry, 1969) consisting of subgrains that are elongated subparallel to adjacent vein-wallrock contacts. Domains of small, nearly strain-free quartz grains occur along grain boundaries and locally along fracture surfaces within the large quartz crystals; these relations closely resemble the

core-and-mantle texture described by White (1976) and Den Brock (1992).

The margins of the vein and areas where the quartz vein pinches consist of finer-grained quartz crystals (Fig. 2b). These crystals are relatively unstrained (some undulose extinction is present), have variable grain sizes ranging from ~0.1–1.0 cm and typically meet at triple points having interfacial angles of ~120°. Domains of crystal aggregates with similar crystallographic orientations occur in the finer-grained areas. In some areas, these domains are nearly optically continuous with larger quartz crystals in the coarse-grained areas described above.

Inclusions of wallrock ~0.5 cm wide and 1.0–2.0 cm long occur in the large quartz vein near vein-wallrock contacts (Fig. 2a,b). The inclusions contain amphibolite facies mineral assemblages. Broken and truncated garnet crystals are present along the inclusion margins (cf. Ague, 1994b).

Intersecting planes of fluid inclusions are widespread in vein quartz. Some planes are confined to individual crystals whereas others transect crystal boundaries. The orientations of the planes are variable but most are approximately perpendicular to adjacent vein-wallrock contacts. The diameters of individual fluid inclusions are ~2 μm or less.

Vein quartz containing planes of minute biotite, muscovite, and, more rarely, kyanite, plagioclase, and staurolite inclusions has been observed in two environments: (1) in zones about 0.5 mm wide directly along the contacts between the large quartz vein and the schist; (2) in the small veinlets that cut the schist. The planes are sub-parallel to the adjacent vein-wallrock contacts and are spaced between about 10 and 100 μm apart. The inclusion plane relations are petrographically identical to the crack-seal textures described by Ramsay (1980).

5.2. Interpretation of Vein Relations

Vein formation must have taken place after garnets began to grow because the vein truncates garnet porphyroblasts. Similar timing relations have been observed throughout the amphibolite facies portion of the Wepawaug Schist (Ague, 1994b). Moreover, the crack-seal areas sometimes contain staurolite and kyanite, which indicates that at least some of the vein growth occurred under amphibolite facies conditions. The crack-seal textures suggest that vein formation was episodic (cf. Ramsay, 1980; Ague, 1994b).

The pinching and swelling of the vein along the fold limbs (Fig. 2) indicates that it was boudinaged during folding. The coarse-grained areas containing the large, strained quartz crystals occur as boudins within the widest parts of the vein. We interpret the textures observed in the finer-grained areas to be the result of dynamic recrystallization (e.g., White, 1976; Den Brock, 1992). Major zones of recrystallization are best developed near vein-wallrock contacts and in pinched regions (boudin necks) of the vein, suggesting that deformation was most intense in these areas. We conclude that the vein was originally composed mostly of coarse-grained quartz and that the finer-grained areas developed as a result of recrystallization associated with folding and boudinage. Vein deformation throughout the amphibolite facies part of the Wepawaug Schist was largely synmetamorphic (Ague, 1994b).

6. RESULTS

The isotopic compositions measured for the traverses and the bulk quartz veins are given in Tables 2–5. The isotopic compositions of quartz in the small veinlets cutting MBW-1 are shown on Figs. 2a and 2b. Mineral compositions are given in Table 6.

6.1. Oxygen Isotope Traverse A-A′

Garnets along Traverse A-A′ show significant isotopic zonation. The $\delta^{18}O$ of garnet cores within and outside the selvage are indistinguishable and average 10.1 ± 0.12‰ (1σ standard error; Fig. 3). The $\delta^{18}O$ of garnet rims outside the selvage is ~10.9‰ (Fig. 3). In contrast, the rims of garnets within the selvage have significantly higher $\delta^{18}O$ of about 11.9‰ (Fig. 3). Thus, the core-to-rim zonation of garnet within selvages is ~1.8‰, whereas outside the selvages it is only ~0.8‰ (Fig. 3).

Variations in the $\delta^{18}O$ of quartz, biotite, kyanite, and plagioclase are relatively small compared to those of garnet (Fig. 3). Muscovite $\delta^{18}O$ may decrease slightly as the vein is approached. In addition, muscovite from one sample outside the selvage (4.5 cm from the major quartz vein) has variable $\delta^{18}O$ that ranges from 12.9–14.0‰ (Fig. 3). The $\delta^{18}O$ of the one staurolite separate that was analyzed is similar to those of kyanite and the rims of garnet within the selvage (Fig. 3).

6.2. Oxygen Isotope Traverse B-B′

Traverse B-B′ extends across the major quartz vein and the aluminous selvage (Fig. 2b, 4). Three of the quartz vein analyses are from an area containing large (cm-scale) crystals; the remainder are from areas composed mostly of finer-grained, recrystallized quartz (Fig. 4). The $\delta^{18}O$ of the vein quartz varies from 15.0–16.4‰; this amount of variability is well in excess of the analytical precision (±0.16‰). No systematic $\delta^{18}O$ variations were apparent as a function of depth within the vein.

The $\delta^{18}O$ of quartz in the adjacent pelitic schist is highly variable and ranges from 14.0–16.3‰ (Fig. 4). $\delta^{18}O$ drops sharply in two areas, one ~2 cm and the other 4.75 cm from the vein-wallrock contact (Fig. 4). The $\delta^{18}O$ of kyanite may also decrease somewhat ~2 cm from the vein but, at present, the robustness of this trend is difficult to judge because of the small number of analyzed samples (N = 2) and the analytical difficulties associated with kyanite. Muscovite and biotite $\delta^{18}O$ for Traverses A-A′ and B-B′ are similar, but the $\delta^{18}O$ of plagioclase from B-B′ is 1–1.5‰ less than that of plagioclase from A-A′.

6.3. Oxygen Isotope Traverses C-C′ and D-D′

Traverse C-C′ lies entirely within a single large crystal of vein quartz (Fig. 5). Two of the analyses of Traverse D-D′ are from a second large crystal, whereas the rest are from a finer-grained, recrystallized area (Fig. 5). The $\delta^{18}O$ of

TABLE 2. OXYGEN ISOTOPE AND LOCATION DATA FOR PELITE, TRAVERSES A-A' AND B-B'

Sample	Location (cm)	Qtz	Ms	Pl	Ky	Stt	Grt rim	Grt core	Bt
				TRAVERSE A-A'					
mbw-1a-1	0.40	-	13.37	-	12.65	-	-	-	10.36
mbw-1a-2	1.20	15.91	13.30	-	-	-	-	-	
mbw-1a-3	1.90	15.28	13.95	-	12.86	-	11.80	10.43	10.11
mbw-1a-4	2.50	15.72	13.84	-	-	12.66	12.08	9.95	-
mbw-1a-5	3.10	15.95	13.54	-	n.p.	n.p.	10.85	10.17	-
	3.10	-	-	-	-	-	10.90	9.91	-
mbw-1a-6	3.70	-	-	12.86	n.p.	n.p.	-	-	-
mbw-1a-7	4.30	15.74	13.95	-	n.p.	n.p.	-	-	-
	4.30	-	12.89	-	-	-	-	-	-
mbw-1a-10	6.10	-	-	13.47	13.05	-	-	-	10.40
mbw-1a-11	6.70	-	-	-	13.07	-	-	-	10.04
				TRAVERSE B-B'					
mbw-1-11	0.75	15.62	-	-	-	-	-	-	-
mbw-1-12	1.25	16.29	-	11.98	-	-	-	-	-
	1.25	16.16	-	-	-	-	-	-	-
mbw-1-13	1.75	14.02	13.47	-	-	-	-	-	10.56
	1.75	14.18	-	-	-	-	-	-	-
mbw-1-15	2.25	14.42	-	-	12.71	-	-	-	10.81
mbw-1-16	2.75	15.46	-	-	-	-	-	-	-
mbw-1-17	3.25	15.66	13.93	-	13.64	-	-	-	10.74
mbw-1-19	4.25	15.95	-	-	-	-	-	-	-
mbw-1-20	4.75	14.20	-	-	-	-	-	-	-

Notes : All analyses are reported in permil with respect to V-SMOW. Location measured from the contact between quartz vein and pelite. n.p. = not present; - = not determined.

the large crystals is remarkably uniform and averages 16.1 ± 0.17‰ (±1σ sample standard deviation). Thus, the crystals are homogeneous within analytical precision. The $\delta^{18}O$ of the crystals is indistinguishable from that of the coarse-grained area investigated in Traverse B-B′ (Fig. 4, 5).

Relative to the large crystals, the isotopic composition of the finer-grained quartz appears to be slightly more variable. $\delta^{18}O$ ranges from 15.6–16.5‰ (Fig. 5).

6.4. Oxygen Isotope Compositions of Veinlets in MBW-1

The isotopic compositions of the four veinlets investigated fall into two groups. The veinlets in the selvages have $\delta^{18}O$ in the range of 15.5–16‰ (Fig. 2a,b). In contrast, the veinlets beyond the selvage margins have much lower $\delta^{18}O$ of 13.8–14.2‰ (Fig. 2a).

6.5. Oxygen Isotope Compositions of Quartz Veins from Other Localities

The $\delta^{18}O$ of quartz from five other veins surrounded by aluminous selvages are given in Table 5 (JAW-122, -125A, -131A, -137B, and W-12). Although the samples were collected over a wide area (Fig. 1), the $\delta^{18}O$ of the vein quartz is surprisingly uniform and varies over a total range of only about 1‰. Furthermore, the average $\delta^{18}O$ of the quartz (16.1‰) is very similar to that of the large quartz vein in sample MBW-1 (Fig. 4) and the wallrock quartz from Traverse A-A′ (Fig. 3).

The isotopic compositions of quartz from veins associated with igneous rocks are 13.1‰ (JvH-W-14) and 12.9‰

TABLE 3. OXYGEN ISOTOPE AND LOCATION DATA FOR VEIN QUARTZ, TRAVERSE B-B'

Sample	Location (cm)	$\delta^{18}O_{Qtz}$
mbw-1-1	-4.250	15.97†
	-4.250	15.83†
	-4.250	16.37†
	-4.250	15.50†
	-4.250	16.21†
mbw-1-2	-3.750	16.04§
	-3.750	15.91#
	-3.750	15.91**
mbw-1-4	-2.925	15.82§
	-2.775	16.20§
mbw-1-5	-2.375	15.78§
	-2.125	16.16§
	-2.125	16.32§
mbw-1-6	-1.750	15.78**
mbw-1-7	-1.250	16.01§
	-1.250	15.03#
	-1.250	16.24**
	-1.250	15.74§
	-1.250	15.70**
mbw-1-8	-0.750	15.33#
	-0.750	15.93§
	-0.750	16.41§
	-0.750	15.74§
	-0.750	15.62§

Notes : All analyses are reported in permil with respect to V-SMOW. Location measured from the contact between quartz vein and pelite; † whole core used for analyses; § top 1/3 of the core used for analyses; # center 1/3 of the core used for analyses; ** bottom 1/3 of the core used for analyses.

TABLE 4. OXYGEN ISOTOPE AND LOCATION DATA FOR VEIN QUARTZ, TRAVERSES C-C' AND D-D'

Sample	Location (cm)	$\delta^{18}O_{Qtz}$
	TRAVERSE C-C'	
mbw-1-2a-1	-3.10	16.29
mbw-1-2a-2	-3.22	15.93
mbw-1-2a-3	-3.30	15.90
mbw-1-2a-4	-3.40	15.90
mbw-1-2a-6	-3.59	16.18
mbw-1-2a-7	-3.67	16.09
mbw-1-2a-10	-4.00	16.30
mbw-1-2a-11	-4.10	15.87
mbw-1-2a-13	-4.29	16.13
	TRAVERSE D-D'	
mbw-1-2b-1	-2.17	15.59
mbw-1-2b-3	-2.38	16.01
mbw-1-2b-5	-2.58	16.46
mbw-1-2b-14	-3.22	15.86
mbw-1-2b-15	-3.30	16.10

Note : All analyses are reported in permil with respect to V-SMOW. Location measured from the contact between quartz vein and pelite.

(JAW-89). These values are significantly lighter than observed for any of the other matrix or vein quartz samples investigated in this study.

7. INTERPRETATION OF RESULTS FOR SAMPLE MBW-1

7.1. Isotopic Equilibrium and Disequilibrium

The isotherm method (Javoy et al., 1970) is a powerful way to assess isotopic equilibrium and disequilibrium between minerals. Our analysis is based on simple fractionation expressions of the form

$$\Delta_{i-j} \sim \frac{A_{i-j} \times 10^6}{T^2}, \quad (1)$$

where i and j denote the mineral phases of interest, A_{i-j} is the equilibrium $^{18}O/^{16}O$ fractionation coefficient for j relative to i, Δ_{i-j} is the equilibrium fractionation between i and j, and T is temperature (K). Equilibrium relations between coexisting minerals are given by linear isotherms:

$$\delta^{18}O_j = a_0 + a_1 A_{i-j}, \quad (2)$$

where a_0 is the y-intercept and a_1 is the slope of the line. It follows that the temperature of equilibration is $T = \sqrt{10^6/|a_1|}$. Because all the rocks studied are quartz-saturated, we take i to be quartz. The success of isotherm analysis depends on the accuracy of the equilibrium fractionation factors (cf. Sharp et al., 1994). To evaluate the errors associated with the A_{Qtz-j}, we did calculations using two independent sets of values. One set (FFI), based largely on field and laboratory calibrations, comprises the expressions of Wenner and Taylor (1971) (chlorite), Bottinga and Javoy (1973) (quartz, plagioclase, muscovite), Bottinga and Javoy (1975) (biotite, ilmenite), Agrinier and Javoy (1988) (rutile), Richter and Hoernes (1988) (staurolite), Lichtenstein and Hoernes (1992) (garnet), and Sharp (1995) (kyanite). The other set (FFII) is based on increment method calculations; it contains the expressions of Zheng (1991) for rutile and ilmenite and Richter and Hoernes (1988) for all other phases.

Several modifications were made to the published fractionation expressions to facilitate the analysis of this section. We used the least-squares method to recast the expressions of Bottinga and Javoy (1973, 1975) for muscovite and biotite to the form of Eqn. 1. The calculations were done for the temperature range appropriate for this study (500–650°C) and resulted in A coefficients of 1.78 for muscovite and 3.27 for biotite. The maximum difference between Δ values calculated using these coefficients and the expressions of Bottinga and Javoy (1973, 1975) is only 0.11‰ for the 500–650°C interval. The fractionation expressions of FFII involve the $A_{i-j} \times 10^6/T^2$ term and two additional terms. We neglected the additional terms because they have little impact on calculated fractionations (±0.1‰) over the 500–650°C range.

By inspection, the data for quartz, muscovite, kyanite, staurolite, and selvage garnet rims from Traverse A-A′ define a reasonably linear array (Fig. 6). We used the least-squares method to fit a line to the data for quartz, muscovite, kyanite, and selvage garnet rims; staurolite is unsuitable for quantitative thermometry because its isotopic properties are poorly known. The mean $\delta^{18}O$ of the phases were weighted according to their respective observed standard errors. The temperature estimates are 599 ± 40°C and 617 ± 40°C for FFI and FFII, respectively ($\pm 2\sigma$; Fig. 6), and are consistent with the peak temperatures of metamorphism estimated by Ague (1994b) using cation exchange thermometry. Thus, we conclude that peak or near-peak temperature isotopic values are preserved for quartz, muscovite, kyanite, and selvage garnet rims from Traverse A-A′. We suggest that staurolite also preserves a peak or near-peak temperature isotopic signature because its $\delta^{18}O$ is reasonably consistent with the best-fit isotherms (Fig. 6).

In contrast, the isotopic compositions of garnet rims outside the selvage, garnet cores, plagioclase, and biotite fall well below the high-temperature isotherms (Fig. 6) and, therefore, are out of equilibrium with quartz, muscovite, kyanite, staurolite, and selvage garnet rims.

Isotopic relations for muscovite, kyanite, and isotopically heavy (~16‰) quartz from Traverse B-B′ are reasonably consistent with the isotherm relations derived for Traverse A-A′ (Fig. 7a) and, thus, suggest equilibration at or near

TABLE 5. BULK QUARTZ VEIN ANALYSES

Sample	Host rock	$\delta^{18}O_{Qtz}$
JvH-W-14 (n = 1)	Aplite (Ky zone)	13.09
JAW-89 (n = 3)	Pelite (Ky zone)	12.87 ± 0.22
JAW-122 (n = 3)	Pelite (Ky zone)	15.50 ± 0.11
JAW-125A (n = 2)	"	16.48 ± 0.22
JAW-131A (n = 2)	Pelite (Stt zone)	16.42 ± 0.09
JAW-137B (n = 2)	Pelite (Ky zone)	16.08 ± 0.27
W-12 (n = 1)	"	15.88

Note : All analyses are reported in permil with respect to V-SMOW.

TABLE 6. MINERAL COMPOSITIONS

	Muscovite			Biotite			Chlorite
	Outside selvage	Selvage	JAW 49*	Outside selvage	Selvage	JAW 49*	JAW-49
Si	3.059	3.095	3.143	2.703	2.732	2.779	2.604
Al^{iv}	0.941	0.905	0.857	1.297	1.268	1.221	0.396
Al^{vi}	1.866	1.858	1.805	0.386	0.426	0.387	1.685
Ti	0.025	0.024	0.018	0.090	0.083	0.089	0.006
$Fe^{\dagger}$	0.051	0.049	0.100	1.055	1.019	1.151	1.060
Mn	0.001	-	0.002	0.005	0.003	0.009	1.228
Mg	0.073	0.077	0.123	1.322	1.297	1.182	0.012
Ba	0.009	0.007	0.005	0.001	0.003	0.001	0.001
Na	0.189	0.178	0.068	0.020	0.021	0.007	0.001
K	0.789	0.786	0.839	0.879	0.897	0.873	0.005
F	-	0.002	0.002	0.055	0.058	0.068	0.001
Cl	0.001	0.001	-	0.001	0.001	0.001	0.002
Total	93.51	94.89	94.43	94.92	95.96	95.76	88.06

	Staurolite		Ilmenite	
	Selvage		MBW-1	JAW-49*
Si	7.732	Ti	0.986	0.998
Ti	0.122	Fe^{2+}	0.958	0.926
Al	18.056	Fe^{3+}	0.041[§]	0.004[§]
$Fe^{\dagger}$	2.527	Mg	0.002	-
Mg	0.527	Mn	0.019	0.072
Mn	0.027	Ca	0.001	-
Ca	0.006			
Zn	0.136			
Total	98.74	Total	99.20	99.29

	Plagioclase			Garnet			
	Outside selvage	Selvage	JAW-49*	Outside selvage[#]	Selvage[#]	Grt rim**	JAW-49*
Si	2.706	2.695	2.860	3.015	3.004	3.002	2.979
Ti	-	-	-	0.004	0.004	0.002	0.003
Al	1.296	1.304	1.138	2.002	2.001	2.014	2.016
$Fe^{\dagger}$	0.000	0.005	0.011	1.985	2.005	2.162	1.965
Mg	-	-	-	0.269	0.273	0.356	0.207
Mn	-	-	-	0.187	0.171	0.118	0.492
Ca	0.279	0.289	0.118	0.517	0.535	0.337	0.346
K	0.003	0.003	0.008	-	-	-	-
Na	0.727	0.718	0.879	-	-	-	-
Total	100.71	100.86	99.85	100.30	100.32	100.46	100.03

Notes: Cations of muscovite and biotite normalized to 11 oxygens. Cations of chlorite, staurolite, ilmenite, plagioclase, and garnet to 14, 47, 3, 8, and 12 oxygens respectively. - = not determined or below detection limit.
* Analyses from Ague (1994b); † all Fe as FeO; § Fe^{3+} based on stoichiometry; # bulk average garnet composition;
** Garnet rim analyses < 5 μm from the rim.

peak temperature conditions. On the other hand, major oxygen isotope disequilibrium is apparent along Traverse B-B′ at a distance of ~2 cm from the quartz vein (Fig. 7b). The $\delta^{18}O$ of quartz in this area is anomalously light—about 14‰. Muscovite, kyanite, and isotopically light quartz define unreasonably high isotherm temperatures >1000°C (Fig. 7b), which strongly suggests that the quartz is out of isotopic equilibrium with the muscovite and kyanite. Quartz-biotite and quartz-feldspar fractionations yield lower apparent temperatures of ~500–700°C (Fig. 7b).

7.2. Thermobarometry

The P and T of equilibration for the selvage assemblage was estimated using: (1) the TWEEQU software of Berman (1991), (2) garnet rim compositions, and (3) the activity models of Berman (1990) (garnet), Chatterjee and Froese (1975) (muscovite), McMullin et al. (1991) (biotite), Furhman and Lindsley (1988) (plagioclase), and Ghiorso (1990) (ilmenite). Rutile, quartz, and kyanite were taken to be pure. Fluid-absent equilibria among the components almandine,

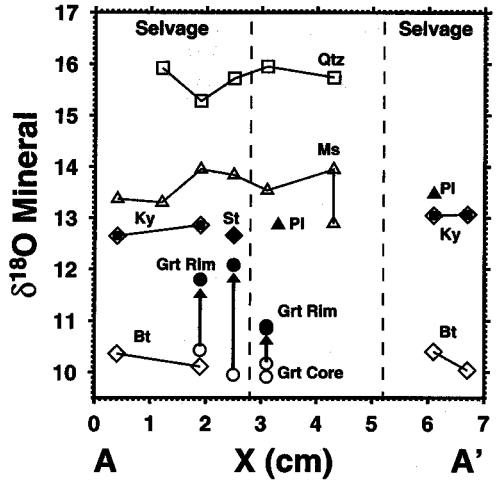

FIG. 3. Oxygen isotope Traverse A-A′. Qtz: quartz; Pl: plagioclase; Ms: muscovite; Ky: kyanite; St: staurolite; Grt: garnet; Bt: biotite (abbreviations after Kretz, 1983). Note that the $\delta^{18}O$ values of garnets within the selvages increase by ~2‰ from core-to-rim.

grossular, pyrope, annite, phlogopite, anorthite, kyanite, quartz, muscovite, rutile, and ilmenite (cf. Table 4 in Berman, 1991) yield a *P-T* estimate of 530 ± 14°C and 0.64 ± 0.05 GPa (±1σ; see Berman, 1991). These values are somewhat less than peak values, which suggests that the minerals equilibrated during exhumation and cooling (cf. Ague, 1994b).

7.3. Isotopic Zonation in Garnet

As shown by Chamberlain and Conrad (1991, 1993), Kohn (1993), Young and Rumble (1993), and Kohn and Valley (1994) oxygen isotope zonation in garnet crystals can preserve a detailed record of fluid infiltration in metamorphic rocks. Garnet is particularly useful because of its large *P-T*

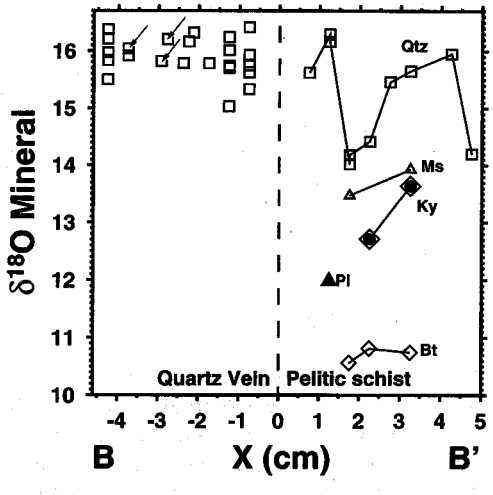

FIG. 4. Oxygen isotope Traverse B-B′. Arrows point to analyses of a single large (1 cm long) crystal of quartz; remainder of vein analyses are from regions composed predominantly of fine-grained, recrystallized quartz.

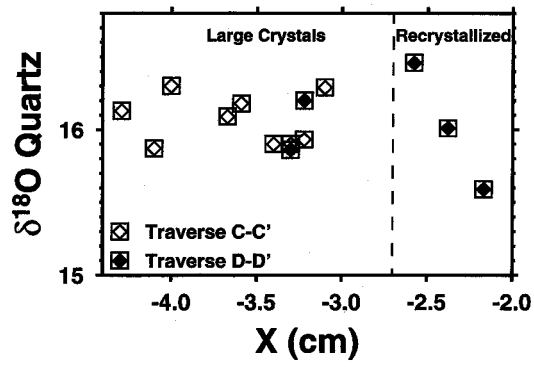

FIG. 5. Oxygen isotope Traverses C-C′ (square with open diamond) and D-D′ (square with filled diamond).

stability field, large crystal size, and extremely low oxygen diffusion coefficient (Coghlan, 1990). In this section we investigate whether the observed isotopic differences between garnet cores and rims (Fig. 6) are consistent with simple models of garnet growth attending prograde metamorphism and dehydration. Two cases are considered: (1) prograde dehydration (cf. Chamberlain and Conrad, 1993; Kohn, 1993) and (2) open-system loss of silica during prograde dehydration.

We used the overall net transfer reaction approach developed by Chamberlain et al. (1990) and Chamberlain and Conrad (1993). The approach requires mass balance such that the $\delta^{18}O$ of a mineral is related to reaction progress by

$$\delta^{18}O_i = \delta^{18}O_{wr} + \sum_{j \neq i} \frac{\nu_j O_j \xi + O_j n_j}{\Sigma_{i \neq j}(O_i n_i) + O_j n_j} \Delta_{i-j}, \quad (3)$$

where wr refers to the whole rock; O_i and O_j are the number of oxygens in one mole of minerals i and j; ν_j is the stoichiometric coefficient of mineral j in the reaction; n_i and n_j are the number of moles of minerals i and j in the rock prior to the reaction; ξ is reaction progress; and Δ_{i-j} is the fraction-

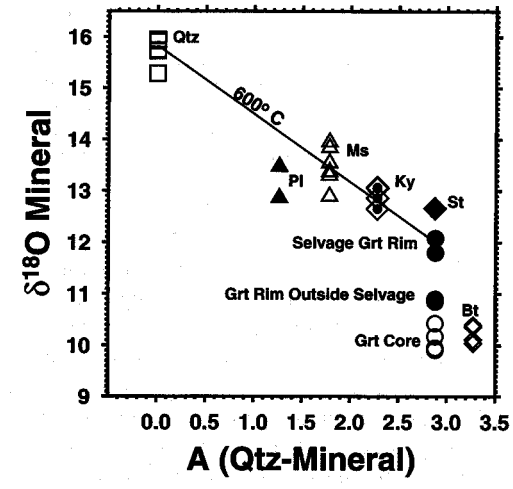

FIG. 6. (a) Isotherm plot using fractionation factor set I (FFI); results for FFII are similar.

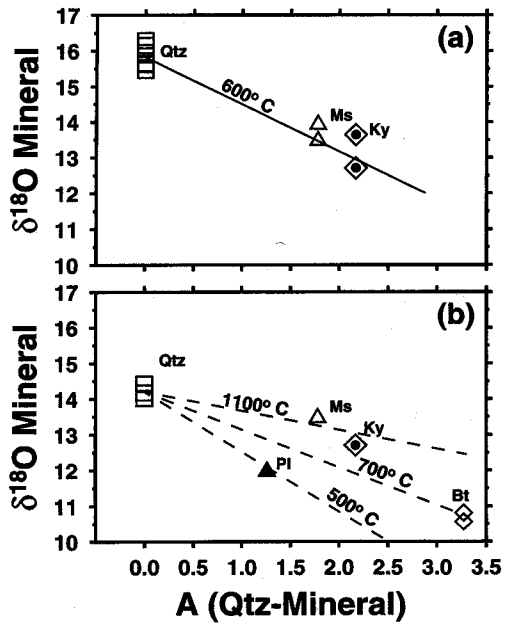

FIG. 7. (a) Isotherm plot for muscovite, kyanite, and isotopically heavy (~16‰) quartz from Traverse B-B′ (FFI). 600°C isotherm for Traverse A-A′ shown for reference. (b) Isotopic systematics for quartz, muscovite, and kyanite in the vicinity of x = 2 cm along Traverse B-B′ (FFI). Plagioclase at x = 1.25 cm also shown. Slopes of 500°C, 700°C, and 1100°C isotherms indicated by dashed lines.

ation between minerals. Following Chamberlain and Conrad (1993), the number of moles of water necessary to fill up the porosity defines one increment of reaction progress. Porosity was set to 0.1% for all calculations (Chamberlain and Conrad, 1993). The water was removed from the system after each step of reaction progress to model the isotopic effects of dehydration. We assumed fractional crystallization of garnet and, therefore, do not include garnet in the calculation of the new whole rock $\delta^{18}O$ after each increment of reaction progress (Chamberlain and Conrad, 1993).

Protolith modal mineralogy and mineral compositions must be well constrained to determine overall net transfer reactions (e.g., Brimhall, 1979; Chamberlain et al., 1990; Ague, 1994b). Sample JAW-49 was chosen as a representative protolith (Ague, 1994a,b). JAW-49, a greenschist facies phyllite, contains tiny (<1 mm diameter) Mn-rich garnets that are interpreted to reflect the initial stages of garnet growth in the metapelitic rocks. The bulk chemistry of JAW-49 is comparable to that of other low-grade metapelitic rocks of the Wepawaug Schist (Ague, 1994a). Ague (1994b) estimated mineral assemblage equilibration conditions of ~0.75 GPa and ~480°C. Mineral compositions for JAW-49 are given in Table 6.

Thermobarometry and field relations indicate that garnet growth started at ~450–500°C and that prograde chlorite had been completely consumed between ~550°C and ~600°C (Ague, 1994a,b). On this basis, we chose 450°C and 600°C as the initial and final model temperatures to determine the maximum likely isotopic zonation in garnet due to prograde reaction in the absence of external fluid infiltration. We make the fundamental assumptions that: (1) the garnet growth rate was linear over this temperature interval and (2) that all minerals were initially in equilibrium with the measured garnet core composition of 10.1‰.

7.3.1. *Case 1: Prograde dehydration*

The zone outside the selvages is the simplest to model because its bulk composition is similar to typical low-grade Wepawaug phyllites and, therefore, it presumably underwent little chemical alteration during metamorphism other than the loss of volatiles. Following Ferry (1984) and Chamberlain and Conrad (1993), we calculated stoichiometric reaction coefficients by subtracting the observed mode of the zone outside the selvages from the calculated mode of the protolith (Table 1). We used the bulk composition of the zone outside the selvages (computed from the modes and mineral analyses of Tables 1 and 6) together with the mineral compositions of JAW-49 to compute the mode for the protolith rock (e.g., Ferry, 1984). We assumed that the protolith mineral assemblage was similar to that observed in rocks just below the garnet isograd (quartz + plagioclase + muscovite + chlorite + biotite + ilmenite + rutile). Graphite and sulfides were ignored (Chamberlain and Conrad, 1993). The resulting whole-rock reaction is

$$1.38\ \mathrm{Bt}^{\circ} + 1.50\ \mathrm{Ms}^{\circ} + 0.30\ \mathrm{Chl} + 1.73\ \mathrm{Pl}^{\circ} + 0.23\ \mathrm{Ilm} \rightarrow 0.89\ \mathrm{Qtz} + 1.75\ \mathrm{Bt}' + 1.21\ \mathrm{Ms}' + 0.45\ \mathrm{Grt}' + 1.53\ \mathrm{Pl}' + 0.07\ \mathrm{Rut} + 1.12\ \mathrm{H_2O}.$$

The superscripts ° and ′ refer to the mineral compositions in the protolith and outside the selvage, respectively.

The calculated increases in the oxygen isotope composition of garnet from core to rim are 0.9‰ and 1.0‰ for fractionation factor sets I and II, respectively (Fig. 8). Furthermore, the model predicts that the $\delta^{18}O$ of quartz should decrease by 0.8–0.9‰ during the course of the reaction. The $\delta^{18}O$ of the whole rock stays nearly constant. The magnitude of the garnet core-to-rim zonation is similar to that predicted by previous models of prograde dehydration reactions (cf. Chamberlain and Conrad, 1993; Kohn, 1993; Young, 1993; Kohn and Valley, 1994).

7.3.2. *Case 2: Open-system silica loss during dehydration*

Aluminous selvages adjacent to veins in the Wepawaug Schist are characterized by major silica depletion caused by the diffusional transport of silica from rocks to fractures (Ague, 1994b). For example, using modal abundance and mineral composition data (Tables 1, 6) we calculate that the molar Si/Al ratios of the selvages and the zone outside the selvages in sample MBW-1 are 1.46 and 3.18, respectively. Under the reasonable assumption that Al was relatively immobile, these ratios indicate that the selvages lost approximately 54% of their silica, relative to the zone outside the selvages (see Ague, 1994a, for calculation methods). This result is similar to that obtained by Ague (1994b) for other selvages.

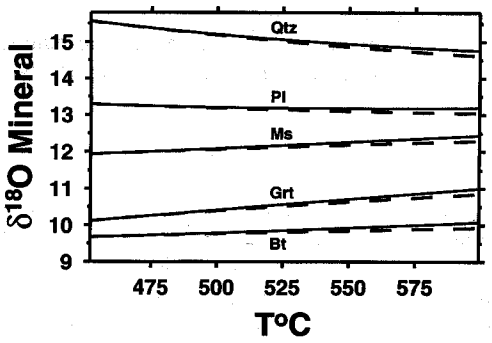

FIG. 8. Isotopic evolution of selected phases during prograde metamorphism predicted using overall net transfer reactions. Solid lines: prograde dehydration (referred to as Case 1 in the text); dashed lines: silica loss and prograde dehydration (Case 2). Results shown are for fractionation factor set I (FFI); results for FFII are similar. Note that the predicted core-to-rim isotopic zonation in garnet is only 0.8–0.9‰.

Because garnet growth and silica loss were largely penecontemporaneous (see above discussion and Ague, 1994b), the effects of open-system silica transport were incorporated into the overall net transfer reaction calculation in order to model the isotopic evolution of garnet in the selvages. To first order, the silica loss can be modeled using a linear rate of silica extraction such that all quartz is removed from the rock when the overall reaction is completed. We assume that (1) no oxygen isotope fractionation occurs between quartz and aqueous silica, (2) the dissolution of quartz is congruent, and (3) the aqueous silica generated during each step of reaction progress cannot react with the rock once it is extracted. We used the overall reaction, temperature range, porosity, and initial oxygen isotopic compositions of Case 1. Thus, the overall reaction can be written as

$$1.38\ \mathrm{Bt}^\circ + 1.50\ \mathrm{Ms}^\circ + 0.30\ \mathrm{Chl} + 1.73\ \mathrm{Pl}^\circ + 0.23\ \mathrm{Ilm} + 14.50\ \mathrm{Qtz} \rightarrow 1.75\ \mathrm{Bt}' + 1.21\ \mathrm{Ms}' + 0.45\ \mathrm{Grt}' + 1.53\ \mathrm{Pl}' + 0.07\ \mathrm{Rut} + 1.12\ \mathrm{H_2O} + 15.40\ \mathrm{SiO_2}\ (\mathrm{aqueous}).$$

We have not considered kyanite and staurolite in the calculations for two reasons. First, the bulk of the isotopic zonation in garnet in rocks of the metamorphic grade and pressure of interest is produced by reactions that consume chlorite, not by reactions involving staurolite and kyanite (cf. Kohn, 1993). Second, petrologic evidence indicates that widespread staurolite and kyanite growth required significant open system fluid infiltration and alkali metal transport (Ague, 1994b). For example, the molar Na/Al ratios of the selvages and the zone outside the selvages are 0.07 and 15, respectively, suggesting that the selvages lost ~55% of their Na during metamorphism.

Results for minerals for Case 2 are shown in Fig. 8. In contrast to Case 1, the $\delta^{18}O$ of the whole rock decreases significantly (by about 1.3‰) during the reaction because of silica removal. Consequently, the amount of isotopic zonation in garnet is less than for Case 1 and amounts to ~0.8‰ from core-to-rim. The $\delta^{18}O$ of quartz, on the other hand, decreases by ~1‰ during the reaction. The small differences in isotopic evolution between Case 1 and Case 2 suggest that local silica loss during prograde dehydration would be difficult to detect using oxygen isotope study alone.

7.3.3. Fluid infiltration and garnet growth

The modeling indicates that the ~2‰ increase from core-to-rim observed for selvage garnets cannot be produced by dehydration reactions proceeding over the maximum likely temperature range in systems that are either closed or open with respect to silica loss and closed with respect to alkalis. Thus, fluid infiltration must have occurred during the growth of selvage garnets (cf. Chamberlain and Conrad, 1993).

On the other hand, the ~0.8‰ core-to-rim increase observed for garnet outside the selvages is consistent with simple models of prograde dehydration without fluid infiltration.

7.4. Equilibration of Oxygen Isotopes During Cooling

Recent studies (e.g., Lasaga, 1983; Giletti, 1986; Eiler et al., 1993) have shown that the chemical and isotopic compositions of coexisting minerals may be reset by diffusion during slow cooling from peak metamorphic conditions. Here, we model this process and compare the results with the oxygen isotope disequilibrium observed for Traverses A-A′ and B-B′. The model is based on the geospeedometry theory of Lasaga (1983); the fast grain boundary approach of Baumgartner and Rumble (1988) and Eiler et al. (1993) is analogous. The calculations assume that intergranular diffusion is instantaneous with respect to intragranular diffusion such that grain boundaries are always in isotopic equilibrium. The interiors of the grains equilibrate with the grain boundaries by volume diffusion. Two different cooling scenarios were investigated. In the first, grain boundary fluid is present throughout the cooling history. In the second, the system becomes dry after a prescribed amount of cooling.

The calculations focus on quartz, plagioclase, muscovite, and biotite and use the modal abundances and grain radii given in Tables 1 and 7. Garnet, staurolite, and kyanite were not considered for three reasons. First, the modal abundances of these phases are relatively low (Table 1). Second, the minerals occur as large porphyroblasts and, thus, their surface area to volume ratios are small. Third, the rates of oxygen self diffusion in garnet are exceedingly low (Coghlan, 1990). Rates of oxygen self diffusion in kyanite and staurolite have yet to be measured. However, diffusion rates in these dense, refractory orthosilicates are also probably very low (cf. Fortier and Giletti, 1989).

In the first set of simulations, the system was cooled from representative peak metamorphic conditions of 600°C to 50°C in 150 Ma such that $1/T(\mathrm{K})$ increased linearly with model time (cf. Eiler et al., 1993). This corresponds to an initial cooling rate of 10°/Ma at 600°C. Results for a wide range of other initial cooling rates (1°/Ma to 100°/Ma) are similar to those presented. The initial isotopic compositions of all phases were calculated using the best-fit isotherms determined above (Fig. 6). Diffusion coefficients (all determined under hydrothermal conditions) are given in Table 7. Because grain boundary fluid was assumed to be present throughout the cooling history, this simulation yields the maximum likely amount of re-equilibration possible.

TABLE 7. GRAIN RADII AND OXYGEN SELF DIFFUSION COEFFICIENTS REFERENCE LIST

	Grain radius		Diffusion coefficient
	Selvage (μm)	Outside selvage (μm)	References
Quartz (wet)	150	120	Farver and Yund (1991)
Albite (wet)	200	125	Giletti et al. (1978)
Muscovite (wet)	260	170	Fortier and Giletti (1991)
Biotite (wet)	300	230	"

The results for both sets of equilibrium fractionation factors (FFI and FFII) are given in Fig. 9a. Because mineral modes and grain sizes influence the evolution of $\delta^{18}O$ during cooling, results for the selvage and the zone outside the selvage differ somewhat from each other. The model predicts that the $\delta^{18}O$ of quartz and plagioclase will increase and the $\delta^{18}O$ of biotite will decrease during cooling (Fig. 9a). The predicted $\delta^{18}O$ for quartz and plagioclase are considerably heavier than measured for either traverse, whereas the predicted $\delta^{18}O$ for biotite is too low (Fig. 9a).

For the second set of simulations, we modeled the situation where grain boundary fluid was present during only the initial stages of cooling from 600°C to 475°C. Diffusion coefficients for dry conditions are unavailable for the micas. However, because rates of oxygen self diffusion in silicates decrease dramatically (usually by several orders of magnitude) under dry conditions (cf. Eiler et al., 1993), we made the reasonable assumption that no significant equilibration occurs below 475°C.

The model system was cooled from 600°C to 475°C in 14.5 Ma such that $1/T(K)$ increased linearly with model time; the initial cooling rate was 10°/Ma at 600°C. Calculated isotopic shifts are considerably less than those predicted for the case of cooling from 600°C to 50°C in the presence of grain boundary fluid (Fig. 9b). On average, biotite displays the largest shift; its $\delta^{18}O$ is predicted to decrease by about 0.8‰ during cooling.

The modeling places several critical constraints on the isotopic evolution of MBW-1. First, the system had to be dry during a large part of the cooling history, otherwise the $\delta^{18}O$ of quartz and feldspar would be significantly higher than observed, whereas the $\delta^{18}O$ of biotite would be significantly lower. Moreover, if hydrothermal fluids were present throughout the cooling, we would expect extensive development of retrograde phases, but these are not observed. Second, model results for the case where fluid is present during only the early stages of cooling are consistent with some of the isotopic systematics of MBW-1, particularly the light $\delta^{18}O$ of biotite observed throughout the rock. Third, diffusional equilibration during cooling cannot account for (1) the anomalously light $\delta^{18}O$ of plagioclase (~12–13.5‰) throughout the rock (Figs. 6, 7), and (2) the isotopically light quartz (~14‰) from veinlets and Traverse B-B′ (Figs. 2a, 4, 7).

8. DISCUSSION

8.1. Regional Fluid Infiltration during Prograde Metamorphism

8.1.1. Prograde infiltration history

External fluids must have infiltrated the aluminous selvages in sample MBW-1 during garnet growth because the amount of isotopic zonation recorded by the garnets is far in excess of that which can be produced by prograde dehydration reactions alone. Selvage growth was a direct consequence of the formation of the large quartz vein that cuts the sample and, thus, the vein was almost certainly the main fluid conduit. Furthermore, fluid advection probably occurred in the adjacent schist because the selvages are cut by veinlets having $\delta^{18}O$ values that are comparable to those of the main vein. The $\delta^{18}O$ of muscovite, kyanite, staurolite, garnet rims, and most of the quartz in the selvages suggest equilibration near peak metamorphic conditions (Fig. 7). These $\delta^{18}O$ values, however, are all ~1‰ too heavy relative to those expected for simple prograde dehydration without infiltration (Fig. 10). We conclude, therefore, that fluid infiltration increased the bulk $\delta^{18}O$ of the selvages. The anomalously light $\delta^{18}O$ of some of the quartz in Traverse B-B′, plagioclase, biotite, and veinlets must have been acquired after this episode of infiltration, as discussed in the following section.

Garnet cores within and outside the selvages have indistinguishable isotopic compositions, which strongly suggests that garnet growth began at the same time throughout the rock. Unlike the selvage garnets, however, the isotopic zonation in garnet beyond the selvage margins is relatively small and consistent with simple models of prograde dehydration and chlorite consumption. Thus, if any infiltration occurred beyond the selvage margins during garnet growth, it was insufficient to cause detectable shifts in bulk $\delta^{18}O$.

Nonetheless, the isotopic relations of Traverse A-A′ strongly suggest that fluid infiltration did occur in the zone outside the selvages. As shown in Fig. 3, the $\delta^{18}O$ of muscovite and quartz inside and outside the selvages are statistically indistinguishable. Moreover, the $\delta^{18}O$ of these phases

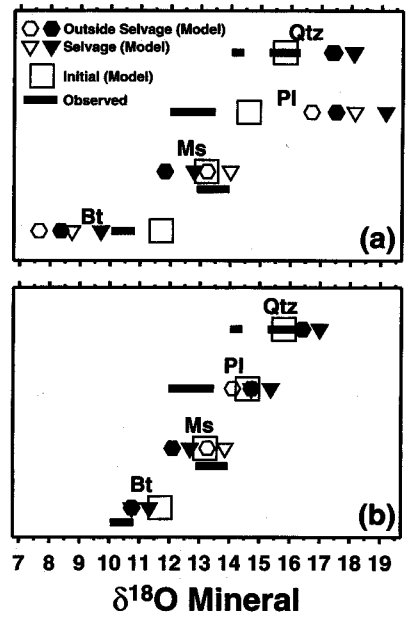

FIG. 9. Predicted isotopic shifts resulting from slow cooling. Open symbols: fractionation factor set I (FFI); filled symbols: FFII. (a) Cooling from 600°C to 50°C in 150 Ma. (b) Cooling from 600°C to 475°C in 14.5 Ma.

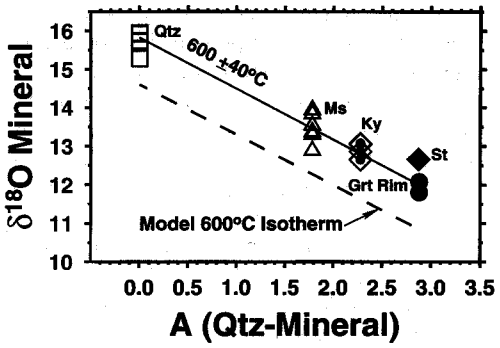

FIG. 10. 600°C isotherm predicted by the overall net transfer model compared to observed $\delta^{18}O$ of quartz, muscovite, kyanite, staurolite, and selvage garnet rims for Traverse A-A'. Note that the observed $\delta^{18}O$ values are all about 1‰ greater than the model isotherm.

are too high (by about 1‰) to be in high temperature equilibrium with the rims of garnet outside the selvages. Consequently, we propose that rock beyond the selvage margins was infiltrated after garnet growth in these areas was largely completed.

8.1.2. *Model*

Based on field and petrologic evidence Ague (1994b, 1995b) concluded that amphibolite facies veins in the Wepawaug Schist were conduits for regional scale, down-temperature fluid outflow. The isotopic data presented here provide a powerful independent test of this conclusion. As shown by Dipple and Ferry (1992) and Steefel (1992), fluid flow along a temperature gradient can result in significant shifts in rock isotopic composition. For an advection-dominated system in which local equilibrium is maintained, isotopic shifts are governed by (Dipple and Ferry, 1992):

$$\delta^{18}O_r'(z) - \delta^{18}O_r^\circ(z) = \delta^{18}O_f^\circ\left(z - \frac{q_m N_f}{V_r}\right) - \delta^{18}O_f^\circ(z), \quad (4)$$

where z is any point along the flow path, N_f is the moles of oxygen per mole of fluid, and V_r is the moles of oxygen per m^3 rock. The superscripts $^\circ$ and $'$ refer to initial and final states whereas the subscripts r and f refer to rock and fluid. For common quartzo-feldspathic rock types, fluid flow down-temperature through a rock mass that initially had the same oxygen isotopic composition everywhere will tend to increase the $\delta^{18}O$ of the rock. The amount of isotopic shift increases in the direction of decreasing temperature along the flow path.

We used Eqn. 4 together with a set of representative initial and boundary conditions to assess whether down-temperature flow could account for the isotope systematics of sample MBW-1. The thermal gradient in the direction of flow was set to −25°/km and the inlet temperature (at $z = 0$ in the lower crust) was 700°C. Our conclusions are little affected by other reasonable assumptions about the temperature gradient and the inlet temperature. The albite-water fractionation expression of Richter and Hoernes (1988) was used to represent the isotopic behavior of the bulk rock. The fluid was assumed to be pure H_2O.

Calculations using Eqn. 4 indicate that a down-temperature flux on the order of 10^4 m^3 m^{-2} would be sufficient to equilibrate the rock with the flowing fluid. The bulk $\delta^{18}O$ of rock at 550–600°C (representative amphibolite facies conditions for the Wepawaug Schist) would increase by about 1‰. This isotopic shift is consistent with that recorded by isotopically zoned garnets in the selvages. Ague (1994b) estimated that the time-integrated fluid flux necessary to form the average amphibolite facies vein was $\sim 3 \times 10^5$ m^3 m^{-2}. This flux was large enough to (1) cause major element metasomatism in the selvages adjacent to the vein (cf. Ague, 1994b) and (2) equilibrate the isotopic composition of the rock with that of the infiltrating fluids. In the zones beyond the selvage margins, most of the infiltration appears to have post-dated garnet growth. Fluxes in these zones were large enough to cause isotopic resetting but were apparently insufficient to cause detectable major element metasomatism.

Of course, incorporation of the effects of diffusion, hydrodynamic dispersion, and the kinetics of fluid-rock interaction will modify the calculation results. Nonetheless, the general result of down-temperature fluid flow under the initial and boundary conditions described above will be to drive the isotopic compositions of rocks to heavier values. It is interesting to note that the isotopic data of Garlick and Epstein (1967) and Chamberlain and Conrad (1993) are consistent with bulk increases in $\delta^{18}O$ during garnet growth elsewhere in the Acadian orogen of New England.

The $\delta^{18}O$ of the bulk of the quartz in MBW-1 (about 16‰) is statistically indistinguishable from the $\delta^{18}O$ of quartz in the other amphibolite facies veins surrounded by selvages that we studied. These relations suggest that a common fluid infiltrated the amphibolite facies schists and that the infiltration was of regional scope.

Advective or diffusive transport across lithologic contacts between rock units of differing initial isotopic composition can propagate isotopic fronts from one rock unit to another (cf. Rye et al., 1976; Bickle, 1992; Chamberlain and Conrad, 1993; Lasaga and Rye, 1993; Kohn and Valley, 1994). With respect to the increases in $\delta^{18}O$ recorded by sample MBW-1, we infer that any role played by front movement was minor because the outcrop area is dominated by pelitic schist and no local source rock for isotopically heavy fluids is present (cf. Palin, 1992).

8.2. Infiltration of Isotopically Light Fluids

8.2.1. *Fluid source*

Plagioclase, biotite, and some of the quartz in MBW-1 have $\delta^{18}O$ values that are significantly lighter (by as much as 2‰) than required for isotopic equilibrium with the fluids that infiltrated during selvage formation (cf. Figs. 6, 7). These $\delta^{18}O$ values can be explained in two ways: (1) relict grains that acquired their low $\delta^{18}O$ prior to the formation of the large quartz vein and its selvage or (2) infiltration of isotopically light fluids after the bulk of vein and selvage formation. These possibilities can be assessed because the

rates of oxygen self diffusion in plagioclase, biotite, and quartz are known. FFI was used for the following calculations; results for FFII are not significantly different.

The $\delta^{18}O$ of plagioclase from Traverse B-B′ (~12‰) is about 2‰ less than expected for equilibrium with selvage-forming fluids. We estimated how long relict plagioclase grains could retain this isotopic composition under amphibolite facies conditions. We computed diffusion profiles assuming that the plagioclase grains: (1) were spherical, (2) had an initial $\delta^{18}O$ of 12‰ ($=\delta^{18}O_i$), and (3) were surrounded by an infinite reservoir of selvage-forming fluid in equilibrium with isotopically heavy (16‰) quartz. Plagioclase surfaces were held in equilibrium with this fluid for all times t ($\delta^{18}O_{eq}$). The solution to the diffusion equation with these initial and boundary conditions is (Carslaw and Jaeger, 1959; Crank, 1975):

$$\frac{\delta^{18}O_r - \delta^{18}O_i}{\delta^{18}O_{eq} - \delta^{18}O_i} = 1 + \frac{2a}{\pi r}\sum_{n=1}^{\infty}\frac{(-1)^n}{n}\sin\frac{n\pi r}{a}\,e^{-Dn^2\pi^2 t/a^2}, \quad (5)$$

where a is the maximum grain radius and $\delta^{18}O_r$ is the $\delta^{18}O$ at radius r. The equilibration time was defined as the time necessary for $(\delta^{18}O_{Bulk}/\delta^{18}O_{eq}) = 0.99$; $\delta^{18}O_{Bulk}$ is the bulk isotopic composition of the grains. Using the diffusion coefficient relation of Giletti et al. (1978) for albite, a representative a of 200 μm, and a reasonable T range of 550°C to 600°C, we calculate that it would take only ~300 years (600°C) to ~600 years (550°C) for the feldspar to equilibrate with the fluid.

Isotopically light quartz ($\delta^{18}O_{Qtz}$ ~14‰) occurs in some of the veinlets (Fig. 2a) and at $x \sim 2$ cm and $x = 4.75$ cm along Traverse B-B′ (Fig. 4). Using Eqn. 5, the diffusion coefficient relation of Farver and Yund (1991), and an a of 150 μm, the estimated time required for diffusional equilibration of 14‰ quartz with selvage-forming fluids ranges from ~4800 years (600°C) to ~37,000 years (550°C).

The calculations for biotite were similar to those described above for plagioclase and quartz, except that a cylindrical geometry was used to represent the biotite crystals (cf. Fortier and Giletti, 1991; Young and Rumble, 1993). The solution to the diffusion equation is (Carslaw and Jaeger, 1959; Crank, 1975):

$$\frac{\delta^{18}O_r - \delta^{18}O_i}{\delta^{18}O_{eq} - \delta^{18}O_i} = 1 - \frac{2}{a}\sum_{n=1}^{\infty}\frac{\exp(-D\alpha_n^2 t)J_0(r\alpha_n)}{\alpha_n J_1(a\alpha_n)}, \quad (6)$$

where r is the radius of the cylinder and J_0 and J_1 are Bessel functions of the indicated order. The α_n are the positive roots of: $J_0(a\alpha) = 0$. The initial composition of the biotite was set to the average value observed for Traverses A-A′ and B-B′ (10.4‰). Using a representative grain radius of 250 μm and the diffusion coefficient relation of Fortier and Giletti (1991), we calculate that it would take ~300 years (600°C) to ~800 years (550°C) for biotite to equilibrate with selvage-forming fluids.

Two lines of evidence suggest that the isotopically light quartz, biotite, and plagioclase grains are not relicts. First, the estimated equilibration times are very short, especially for plagioclase and biotite. We consider it unlikely that relict grains could preserve their isotopic compositions throughout the amphibolite facies metamorphism given the large time-integrated fluid fluxes involved in vein formation (~3×10^5 m^3 m^{-2}) and the probable duration of the Acadian orogeny (~10^7 years). Furthermore, if deformation and recrystallization of grains was taking place during fluid infiltration, which is likely, then the timescales for equilibration would be less than predicted by simple diffusion models. Second, Palin (1992) measured the $\delta^{18}O$ of quartz in metapelitic rocks at several lower and middle greenschist facies sites in the Wepawaug Schist. None of the quartz in these rocks has $\delta^{18}O$ as low as the ~14‰ values found in MBW-1.

It is probable, therefore, that MBW-1 was infiltrated by isotopically light fluids after the bulk of the vein and selvage formation was finished. The deep level of metamorphism (>25 km) argues against the infiltration of unmodified, ^{18}O-depleted meteoric fluids. The quartz from veins associated with leucocratic igneous rocks (JvH-W-14, JAW-89; Table 5) have $\delta^{18}O$ of ~13‰—the lowest quartz $\delta^{18}O$ measured in this study. On this basis, we suggest that the isotopically light fluids were derived from the widespread pods and dikes of leucocratic igneous rocks that intruded the schists. Several of these intrusions are exposed in the vicinity of the MBW-1 outcrop (cf. Fig. 1 and Fritts, 1965a). Most of the intrusive activity occurred during amphibolite facies metamorphism (Ague, 1994b), which implies temperatures of fluid infiltration between about 550 and 600°C. We note that the amphibolite facies quartz vein cutting the marble studied by Tracy et al. (1983) also has $\delta^{18}O$ of ~13‰. Consequently, we infer that the vein-related isotopic and chemical metasomatism documented by Tracy et al. (1983) resulted from infiltration of "magmatic fluids".

The low $\delta^{18}O$ of biotite could have resulted from: (1) interaction of biotite with low $\delta^{18}O$ fluids, and/or (2) diffusional oxygen isotope exchange with matrix phases during cooling under conditions where grain boundary fluids were present during the early part of the cooling history (Fig. 9b). We are unable to distinguish between these two possibilities at present.

8.2.2. *Duration and mechanisms of fluid-rock interaction*

Isotopic relationships among plagioclase, quartz, and muscovite at $x \sim 2$ cm along Traverse B-B′ provide constraints on the duration and mechanisms of fluid-rock interaction. We investigated the timescales necessary for diffusional equilibration of muscovite with isotopically light fluids using Eqn. 6. We assumed (1) a grain radius of 250 μm, (2) that the muscovite surfaces were in equilibrium with an infinite reservoir of isotopically light fluid, and (3) that the fluid was in equilibrium with isotopically light quartz ($\delta^{18}O_{Qtz}$ = 14‰). The initial composition of the muscovite was set to 13.5‰ based on the 600°C FFI isotherm relations of Fig. 6. With these initial and boundary conditions and the diffusion coefficient relation of Fortier and Giletti (1991), we calculate that it would take ~700 years (600°C) to ~2600 years (550°C) for muscovite to equilibrate with the fluid and attain a final $\delta^{18}O$ of ~11.5‰.

The equilibration time for quartz at these temperatures

(see above) is about 7–14 times greater than that for muscovite. Thus, if quartz equilibrated with the isotopically light fluids by diffusion alone, we would expect that the isotopic composition of muscovite would also be decreased significantly. The $\delta^{18}O$ of the muscovite is, however, about 1.5–2.5‰ greater than the ~11.5‰ value predicted for equilibration with the isotopically light fluids. Thus, no clear evidence exists for the interaction of muscovite with isotopically light fluids. It follows that the low $\delta^{18}O$ quartz attained its isotopic composition by precipitation, mineral reaction, or recrystallization in the presence of such fluids, not by slow diffusional equilibration. On the other hand, diffusion-controlled modification of plagioclase and biotite $\delta^{18}O$ may have occurred because of the very short times required for equilibration of these phases.

The calculations suggest that the timescales of fluid-rock interaction were short: probably 10^3–10^4 years. Similar short timescales were calculated by Young and Rumble (1993) for fluid-rock interaction in a sample of Gassetts Schist from Vermont. The total duration of fluid flow may have exceeded 10^3–10^4 years because the calculations do not take episodic fluid flow into account.

We suggest that the selvages and the regions beyond the selvages in MBW-1 were infiltrated pervasively because all analyzed plagioclase apparently exchanged oxygen with isotopically light fluids. Most of the precipitation/recrystallization processes forming isotopically light quartz, however, appear to have been restricted to more discrete, mm-scale regions such as veinlets. The isotopically light veinlets were probably regions of high fluid flux during the infiltration.

Some of the quartz samples from the major quartz vein cutting MBW-1 have $\delta^{18}O$ in the range 15–15.3‰ (Fig. 4). These values are intermediate between the light values (~14‰) observed in some veinlets and along Traverse B-B′ and the heavier values (~16‰) that characterize the bulk of the vein and the surrounding pelitic schist. We suggest that the 15–15.3‰ values reflect varying degrees of interaction of pre-existing ~16‰ quartz with isotopically light fluids. The interaction probably occurred during deformation of the vein because the 15–15.3‰ quartz is found in recrystallized regions.

9. SUMMARY AND CONCLUSIONS

The isotopic results presented here provide unique constraints on mechanisms and timescales of fluid-rock interaction during amphibolite facies metamorphism of pelitic schist at middle to lower crustal levels. The petrogenesis of Wepawaug Schist sample MBW-1 involved multiple fluid infiltration events that affected significantly the isotopic and chemical composition of the rock.

9.1. Vein and Selvage Formation

The fracturing and mass transfer that produced the large (2–6 cm wide) quartz vein (Fig. 2) was initiated after garnets began to grow. Zones of aluminous altered wallrock (selvages) characterized by low Si/Al and low Na/Al developed adjacent to the vein during vein growth (cf. Ague, 1994b). Garnets in the selvages record nearly 2‰ increases in $\delta^{18}O$ from core-to-rim. Modeling of likely prograde reaction histories indicates that this amount of core-to-rim zonation required infiltration of external fluids that increased the $\delta^{18}O$ of the bulk selvage during garnet growth. Isotopic zonation in garnet beyond the selvage margins is <1‰ from core-to-rim and is consistent with prograde reaction with little or no infiltration of external fluids. We suggest, therefore, that the selvages were zones of significant infiltration and that the quartz vein was the major fluid conduit. In addition, some infiltration probably occurred beyond the selvage margins after garnets in these areas had largely finished growing.

Petrologic studies (Ague, 1994b) strongly suggest that quartz vein formation required channelized fluid flow down regional temperature and pressure gradients. The time-integrated fluid flux necessary to form the average amphibolite facies vein was estimated to be $\sim 3 \times 10^5$ m^3 m^{-2} by Ague (1994b). Isotopic modeling assuming local fluid-rock equilibrium and advection-dominated flow (Dipple and Ferry, 1992) indicates that down-temperature fluxes of this magnitude would be sufficient to increase the bulk isotopic compositions of pelitic rocks, consistent with our isotopic results. The isotopic compositions of quartz veins surrounded by selvages at five other amphibolite facies localities throughout the schist are statistically indistinguishable from that of the MBW-1 vein, which suggests that the fluid infiltration and chemical and isotopic mass transfer was regional in scope. Thus, we conclude that major, channelized outflow of metamorphic fluids occurred through the amphibolite facies portion of the Wepawaug Schist.

9.2. Infiltration of Low $\delta^{18}O$ Fluids

While still under amphibolite facies conditions but after the bulk of the vein and its selvages had formed, the rock was pervasively infiltrated by fluids with $\delta^{18}O$ significantly lighter (by about 2‰) than required for high-temperature isotopic equilibrium with vein quartz and matrix minerals. The $\delta^{18}O$ of plagioclase throughout the rock was decreased by these fluids. Quartz crystallized or recrystallized in the presence of the fluids in narrow (mm scale) zones and veinlets within the rock matrix and in deformed areas within the major quartz vein. The $\delta^{18}O$ of muscovite, however, does not appear to have been affected significantly by the infiltration, which suggests short timescales of fluid-rock interaction on the order of 10^3–10^4 years. The total duration of flow may have been longer than this because our calculations do not take episodic flow into account. Quartz veins associated with the dikes and pods of synmetamorphic leucocratic igneous rocks that intruded the amphibolite facies portion of the Schist have low $\delta^{18}O$ of ~13‰. On this basis, we conclude that the isotopically light fluids that infiltrated MBW-1 were derived from crystallizing intrusions. Similar fluids infiltrated other rocks in the area, including the marble studied by Tracy et al. (1983).

Acknowledgments—We thank A. C. Lasaga, M. Davis, J. Feehan, J. Hicks, Jose-Luis Mogollon, U. Ring, and J. Soler for stimulating scientific discussions, C. P. Chamberlain, J. M. Ferry, and an anonymous referee for critical and constructive reviews, and B. R. Frost for thoughtful comments and editorial handling. Financial support

from National Science Foundation grants EAR-918006 and EAR-9405889 and Department of Energy grant DE-FG02-90ER14153 is gratefully acknowledged.

Editorial handling: B. R. Frost

REFERENCES

Ague J. J. (1994a) Mass transfer during Barrovian metamorphism of pelites, south-central Connecticut, I: Evidence for changes in composition and volume. *Amer. J. Sci.* **294,** 989–1057.

Ague J. J. (1994b) Mass transfer during Barrovian metamorphism of pelites, south-central Connecticut, II: Channelized fluid flow and the growth of staurolite and kyanite. *Amer. J. Sci.* **294,** 1061–1134.

Ague J. J. (1995a) Deep crustal growth of quartz, kyanite, and garnet into large-aperture, fluid-filled fractures, north-eastern Connecticut, USA. *J. Metam. Geol.* **13,** 299–314.

Ague J. J. (1995b) Mass transfer during Barrovian metamorphism of pelites, south-central Connecticut, Reply. *Amer. J. Sci.* **295,** 1025–1033.

Agrinier P. and Javoy M. (1988) A natural calibration of the quartz-rutile mineral pair oxygen isotope geothermometer. *Chem. Geol.* **70,** 182 (abstr.).

Armstrong T. R., Tracy R. J., and Hames W. E. (1992) Contrasting styles of Taconian, eastern Acadian and western Acadian metamorphism, central and western New England. *J. Metam. Geol.* **10,** 415–426.

Bailey E. H. and Stevens R. E. (1960) Selective staining of K-Feldspar and plagioclase on rock slabs and thin sections. *Amer. Mineral.* **45,** 1020–1025.

Baumgartner L. P. and Rumble D. (1988) Transport of stable isotopes. I: Development of a kinetic continuum theory for stable isotope transport. *Contrib. Mineral. Petrol.* **98,** 417–430.

Berman R. G. (1990) Mixing properties of Ca-Mg-Fe-Mn garnets. *Amer. Mineral.* **75,** 328–344.

Berman R. G. (1991) Thermobarometry using multi-equilibrium calculations: A new technique, with petrological applications. *Canadian Mineral.* **29,** 833–855.

Bickle M. J. and McKenzie D. (1987) The transport of heat and matter by fluids during metamorphism. *Contrib. Mineral. Petrol.* **95,** 384–392.

Bickle M. J. (1992) Transport mechanisms by fluid-flow in metamorphic rocks: oxygen and strontium decoupling in the Trois Seigneurs Massif: a consequence of kinetic dispersion? *Amer. J. Sci.* **292,** 289–316.

Bottinga Y. and Javoy M. (1973) Comments on oxygen isotope geothermometry. *Earth Planet. Sci. Lett.* **20,** 250–265.

Bottinga Y. and Javoy M. (1975) Oxygen isotope partitioning among minerals in igneous and metamorphic rocks. *Rev. Geophys. Space Phys.* **13,** 401–418.

Brimhall G. H., Jr. (1979) Lithologic determination of mass transfer mechanisms of multiple-stage porphyry copper mineralization at Butte, Montana: Vein formation by hypogene leaching and enrichment of potassium silicate protore. *Econ. Geol.* **74,** 556–589.

Carslaw H. S. and Jaeger J. C. (1959) *Conduction of Heat in Solids.* Oxford Univ. Press.

Chamberlain C. P. and Conrad M. E. (1991) Oxygen isotope zoning in garnet. *Science* **254,** 403–406.

Chamberlain C. P. and Conrad M. E. (1993) Oxygen-isotope zoning in garnet: A record of volatile transport. *Geochim. Cosmochim. Acta* **57,** 2613–2629.

Chamberlain C. P. and Rumble D., III (1988) Thermal anomalies in a regional metamorphic terrane: An isotopic study of the role of fluids. *J. Petrol.* **29,** 1215–1232.

Chamberlain C. P., Ferry J. M., and Rumble D., III (1990) The effect of net transfer reactions on the isotopic composition of minerals. *Contrib. Mineral. Petrol.* **105,** 322–336.

Chatterjee N. D. and Froese E. (1975) A thermodynamic study of the pseudobinary join muscovite-paragonite in the system $KAlSi_3O_8$-$NaAlSi_3O_8$-Al_2O_3-SiO_2-H_2O. *Amer. Mineral.* **60,** 985–993.

Clayton R. N. and Mayeda T. K. (1963) The use of bromine pentafluoride in the extraction of oxygen from oxides and silicates for isotopic analyses. *Geochim. Cosmochim. Acta* **27,** 43–52.

Coghlan R. A. (1990) Studies in diffusional transport: grain boundary transport of oxygen in feldspars, diffusion of oxygen, strontium, and the REEs in garnet, and thermal histories of granitic intrusions in south-central Maine using oxygen isotopes. Ph.D. dissertation, Brown Univ.

Crank J. (1975) *The Mathematics of Diffusion.* Oxford Univ. Press.

Den Brock B. (1992) An experimental investigation into the effect of water on the flow of quartzite. *Geol. Ultraiectina* **95.**

Dieterich J. H. (1968) Sequence and mechanisms of folding in the area of New Haven, Naugatuck, and Westport, Connecticut. Ph.D. dissertation, Yale Univ.

Dipple G. M. and Ferry J. M. (1992) Fluid flow and stable isotopic alteration in rocks at elevated temperatures with applications to metamorphism. *Geochim. Cosmochim. Acta* **56,** 3539–3550.

Eiler J. M., Valley J. W., and Baumgartner L. P. (1993) A new look at stable isotope thermometry. *Geochim. Cosmochim. Acta* **57,** 2571–2583.

Farver J. R. and Yund R. A. (1991) Oxygen diffusion in quartz: Dependence on temperature and water fugacity. *Chem. Geol.* **90,** 55–70.

Ferry J. M. (1984) A biotite isograd in south-central Maine, USA: Mineral reactions, fluid transfer, and heat transfer. *J. Petrol.* **25,** 871–893.

Ferry J. M. (1992) Regional metamorphism of the Waits River Formation, eastern Vermont, delineation of a new type of giant metamorphic hydrothermal system. *J. Petrol.* **33,** 45–94.

Ferry J. M. and Dipple G. M. (1991) Fluid flow, mineral reactions, and metasomatism. *Geology* **19,** 211–214.

Fortier S. M. and Giletti B. J. (1989) An empirical model for predicting diffusion coefficients in silicate minerals. *Science* **245,** 1481–1484.

Fortier S. M. and Giletti B. J. (1991) Volume self-diffusion of oxygen in biotite, muscovite, and phlogopite micas. *Geochim. Cosmochim. Acta* **55,** 1319–1330.

Fritts C. E. (1962) Age and sequence of metasedimentary and metavolcanic formations northwest of New Haven. *USGS Prof. Paper 450-D,* 32–36.

Fritts C. E. (1963) Bedrock geology of the Mount Carmel quadrangle, Connecticut. USGS Quadrangle Map GQ-199.

Fritts C. E. (1965a) Bedrock geology of the Ansonia quadrangle, Fairfield and New Haven Counties, Connecticut. USGS Quadrangle Map GQ-426.

Fritts C. E. (1965b) Bedrock geology of the Milford quadrangle, Fairfield and New Haven Counties, Connecticut. USGS Quadrangle Map GQ-427.

Fuhrman M. L. and Lindsley D. H. (1988) Ternary feldspar modelling and thermometry. *Amer. Mineral.* **73,** 201–215.

Garlick G. D. and Epstein S. (1967) Oxygen isotope ratios in coexisting minerals of regionally metamorphosed rocks. *Geochim. Cosmochim. Acta* **31,** 124–181.

Gates O. (1975) Geologic map and cross-section of the Eastport Quadrangle, Washington County, Maine. Maine Geological Survey, Geology Map Series 3, scale 1:62,500.

Ghiorso M. S. (1990) Thermodynamic properties of hematite-ilmenite-geikielite solid solutions. *Contrib. Mineral. Petrol.* **104,** 645–667.

Giletti B. J. (1986) Diffusion effects on oxygen isotope temperatures of slowly cooled igneous and metamorphic rocks. *Earth Planet. Sci. Lett.* **89,** 115–122.

Giletti B. J., Semet M. P., and Yund R. A. (1978) Studies in diffusion III. Oxygen in feldspars, an ion microprobe determination. *Geochim. Cosmochim. Acta* **42,** 45–57.

Hewitt D. A. (1973) The metamorphism of micaceous limestones from south-central Connecticut. *Amer. J. Sci.* **273-A,** 444–469.

Hewitt D. A. and Wones D. R. (1975) Physical properties of some synthetic Fe-Mg-Al trioctahedral biotites. *Amer. Mineral.* **60,** 444–467.

Hoisch T. D. (1991) The thermal effects of pervasive and channelized fluid flow in the deep crust. *J. Geol.* **99,** 69–80.

Holdaway M. J., Mukhopadhyay B., and Dutrow B. L. (1995) Ther-

modynamic properties of stoichiometric staurolite $H_2Fe_4Al_{18}Si_8O_{48}$ and $H_6Fe_2Al_{18}Si_8O_{48}$. *Amer. Mineral.* **80,** 520–533.

Javoy M., Fourcade S., and Allegre C. J. (1970) Graphical method for examination of $^{18}O/^{16}O$ fractionations in silicate rocks. *Earth Planet. Sci. Lett.* **10,** 12–16.

Kohn M. J. (1993) Modeling of prograde mineral $\delta^{18}O$ changes in metamorphic systems. *Contrib. Mineral. Petrol.* **113,** 249–261.

Kohn M. J. and Valley J. W. (1994) Oxygen-isotope constraints on metamorphic fluid flow, Townshend dam, Vermont, USA. *Geochim. Cosmochim. Acta* **58,** 5551–5566.

Kretz R. (1983) Symbols for fock-forming minerals. *Amer. Mineral.* **68,** 277–279.

Lanzirotti A. and Hanson G. N. (1992) Multiple generations of monazite growth in the Wepawaug Schist, southern Connecticut. *GSA Abstr. Prog.* **24,** A219 (abstr.).

Lanzirotti A., Hanson G. N., and Smith R. D. (1995) The Orange-Milford Belt of Southwestern Connecticut: Identifying unique crustal packages in New England using combined geochemistry, geochronology, and petrology. *GSA Abstr. Prog.* **27-1,** 63 (abstr.).

Lasaga A. C. (1983) Geospeedometry: An extension of geothermometry. In *Kinetics and Equilibrium in Mineral Reactions* (ed. S. K. Saxena); *Adv. Phys. Geochem.* **3,** 81–114. Springer Verlag.

Lasaga A. C. and Rye D. M. (1993) Fluid flow and chemical reaction kinetics in metamorphic systems. *Amer. J. Sci.* **293,** 361–404.

Lichtenstein U. and Hoernes S. (1992) Oxygen isotope fractionation between grossular-spessartine garnet and water: An experimental investigation. *Eur. J. Mineral.* **4,** 239–249.

McMullin D. W. A., Berman R. G., and Greenwood H. J. (1991) Calibration of the SGAM thermobarometer for pelitic rocks using data from phase-equilibrium experiments and natural assemblages. *Canadian Mineral.* **29,** 889–908.

McOnie A. W., Fawcett J. J., and James R. S. (1975) The stability of intermediate chlorites of the clinochlore-daphnite series at 2 kbar. *Amer. Mineral.* **60,** 1047–1062.

Osberg P. H., Tull J. F., Robinson P., Hon R., and Butler J. R. (1989) The Acadian Orogeny. In *The Appalacian-Ouachita Orogen in the United States* (ed. R. D. Hatcher, Jr., et al.), pp. 179–232. Geol. Soc. America.

Palin J. M. (1992) Stable isotope studies of regional metamorphism in the Wepawaug Schist, Connecticut. Ph.D. dissertation, Yale Univ.

Palin J. M. and Rye D. M. (1992) Direct comparison of mineralogic and stable isotopic records of metamorphic fluid flow. *GSA Abstr. Prog.* **24,** A172 (abstr.).

Palin J. M. and Seidemann D. E. (1990) Intergranular control of argon and oxygen isotope transport in metamorphic rocks: Implications for cooling rate studies. *2nd V. M. Goldschmidt Conf. Prog. Abstr.,* p. 71 (abstr.).

Ramsay J. G. (1980) The crack-seal mechanism of rock deformation. *Nature* **284,** 135–139.

Richter R. and Hoernes S. (1988) The application of the increment method in comparison with experimentally derived and calculated O-isotope fractionations. *Chem. Erde* **48,** 1–18.

Rodgers J. (1985) Bedrock Geological Map of Connecticut. Connecticut Geological and Natural History Survey, Department of Environmental Protection, Scale 1:125,000.

Rye R. O., Schuiling R. D., Rye D. M., and Jansen J. B. H. (1976) Carbon, hydrogen, and oxygen isotope studies of the regional metamorphic complex at Naxos, Greece. *Geochim. Cosmochim. Acta* **40,** 1031–1049.

Schnabel R. W. (1975) Geologic map of the New Hartford quadrangle, northwestern Connecticut. USGS Quadrangle Map GQ-1257.

Sharp Z. D. (1995) Oxygen isotope geochemistry of the Al_2SiO_5 polymorphs. *Amer. J. Sci.* **295,** 1058–1076.

Sharp Z. D., Essene E. J., and Hunziker J. C. (1994) Stable isotope geochemistry and phase equilibria of coesite-bearing whiteschists, Dora Maira Massif, western Alps. *Contrib. Mineral. Petrol.* **114,** 1–12.

Spry A. (1969) *Metamorphic Textures.* Pergamon.

Steefel C. I. (1992) Coupled fluid flow and chemical reaction: Model development and application to water-rock interaction. Ph.D. dissertation, Yale Univ.

Taylor H. P., Albee A. L., and Epstein S. (1962) The relationship between $^{18}O/^{16}O$ ratios in coexisting minerals of igneous and metamorphic rocks. *Geol. Soc. Amer. Bull.* **73,** 461–480.

Tracy R. J., Rye D. M., Hewitt D. A., and Schiffries C. M. (1983) Petrologic and stable isotopic studies of fluid-rock interactions, south-central Connecticut: I. The role of infiltration in producing reaction assemblages in impure marbles. *Amer. J. Sci.* **283-A,** 589–616.

Vidale R. J. (1974) Vein assemblages and metamorphism in Dutchess County, New York. *Geol. Soc. Amer. Bull.* **85,** 303–306.

Walther J. V. and Orville P. M. (1982) Volatile production and transport in regional metamorphism. *Contrib. Mineral. Petrol.* **79,** 252–257.

Walther J. V. and Holdaway M. J. (1995) Mass transfer during Barrovian metamorphism. *Amer. J. Sci.* **295,** 1020–1025.

Wenner D. B. and Taylor H. P., Jr (1971) Temperatures of serpentinization of metamorphic rocks based upon $^{18}O/^{16}O$ fractionation between coexisting serpentine and magnetite. *Contrib. Mineral. Petrol.* **32,** 165–185.

White S. H. (1976) The effects of strain on the microstructures, fabrics, and deformation mechanisms in quartzites. *Phil. Trans. Roy. Soc. London A.* **283,** 69–86.

Yardley B. W. D. (1975) On some quartz-plagioclase veins in the Connemara schists, Ireland. *Geol. Mag.* **112,** 183–190.

Yardley B. W. D. (1986) Fluid migration and veining in the Connemara schists, Ireland. In *Fluid-rock Interactions During Metamorphism* (ed. J. V. Walther and B. J. Wood), pp. 109–131. Springer-Verlag.

Yardley B. W. D. and Bottrell S. H. (1992) Silica mobility and fluid movement during metamorphism of the Connemara schists, Ireland. *J. Metam. Geol.* **10,** 453–464.

Young E. D. (1993) On the $^{18}O/^{16}O$ record of reaction progress in open and closed metamorphic systems. *Earth Planet. Sci. Lett.* **117,** 147–167.

Young E. D. and Rumble D., III (1993) The origin of correlated variations in in-situ $^{18}O/^{16}O$ and elemental concentrations in metamorphic garnet from southeastern Vermont, USA. *Geochim. Cosmochim. Acta* **57,** 2585–2597.

Zheng Y-F (1991) Calculation of oxygen isotope fractionation in metal oxides. *Geochim. Cosmochim. Acta* **55,** 2299–2307.